2013

Myelin is not required for maintenance of the axon initial segment

Anna Josephson
Virginia Commonwealth University

MYELIN IS NOT REQUIRED FOR THE MAINTENANCE OF THE AXON INITIAL SEGMENT

A thesis submitted in partial fulfillment of the requirements for the degree of Master of Science at Virginia Commonwealth University.

by

ANNE MARIE JOSEPHSON
Bachelor of Science in Biology, James Madison University, 2011

Director: JEFFREY L. DUPREE, PH.D.
ASSOCIATE PROFESSOR OF ANATOMY AND NEUROBIOLOGY

Virginia Commonwealth University
Richmond, Virginia
May, 2013

Acknowledgement

I would first like to express my sincere gratitude to my advisor, Dr. Dupree, for his endless patience, enthusiasm, support and immense knowledge. Under his guidance I have become a better researcher. I thank him for always challenging me to think critically and innovatively. His commitment to my success was invaluable. It has truly been a privilege to work in his lab.

I would also like to thank Dr. Henderson, Director of the Microscopy Facility, for his direction and time spent with me on the microscope. His assistance and expertise on microscopy and computer software was instrumental in the completion of this project. I would also like to extend my appreciation to the rest of my committee, Dr. Colello, Dr. DeVries and Dr. Oh, for their time, encouragement and insightful comments.

Apart from my committee members, I would like to extend my gratitude to Dr. Fuss for generously purchasing the mice and Dr. Morgan for preparing them for my experiments.

In addition, I would like to express my thanks to my fellow lab members, Afua Andoh and Clay Behl, for their assistance on this project and to my remaining lab members, Jacqueline DeLoyht, Carine Binyam and Kareem Clark, for their support and reassurance.

Finally, I would like to thank my family and friends for their unconditional love and unending support.

Table of Contents

List of Tables

Page

List of Figures

Page

List of Abbreviations

AIS……axon initial segment

AP……..……action potential

ankG……ankyrinG

APP……Amyloid Precursor Protein

BBB……Blood-brain barrier

Ca^{2+}……Calcium ion

CAM……..cell adhesion molecule

Caspr……contactin-associated protein

Caspr2……..CAM contactin-associated protein 2

CGT……..galactose-ceramide galactosyltransferase

CM……compact myelin

CNP……2':3'-cyclic nucleotide 3'-phosphodiesterase

CNS……..central nervous system

ECM……..extracellular matrix

GalC……galactocerebroside

K^+……potassium ion

K_v……..voltage-gated potassium channel

MAG……myelin-associated glycoprotein

MBP…….myelin basic protein

MCAO……middle cerebral artery occlusion

MOG……..myelin-oligodendrocyte protein

MS…….Multiple sclerosis

Na……..Sodium

Na^+……..Sodium ion

NaCl…….Sodium chloride

Na_V……voltage-gated sodium channel

NF-155…….neurofascin-155

NF-186…….neurofascin-186

NrCAM……..neural cell adhesion molecule

OCT……Optimal Cutting Temperature

PBS……..phosphate buffered saline

PLP……..proteolipid protein

PNL……..perinodal cytoplasmic loops

PNS…….peripheral nervous system

TAG-1…….transient axonal glycoprotein-1

TMEV……..Theiler's Murine Encephalomyelitis Virus

TO……..Theiler's original

µm…….micron

Abstract

DETERMINING THE ROLE OF MYELIN IN MAINTAINING AXON INITIAL SEGMENT STABILITY

By Anne Marie Josephson, B.S.

A thesis submitted in partial fulfillment of the requirements for the degree of Master of Science at Virginia Commonwealth University.

Virginia Commonwealth University, 2013.

Major Director: Jeffrey L. Dupree, Ph.D.
Associate Professor of Anatomy and Neurobiology

Axonal pathology is a major contributor to impaired motor, sensory and cognitive dysfunction associated with multiple sclerosis particularly with the progressive forms of the disease. However, the early pathologic events responsible for axonal deterioration remain unclear. It is well recognized that maintaining proper axonal function is intimately related to proper establishment and maintenance of axonal domains such as the node of Ranvier and the axon initial segment (AIS). Numerous laboratories, including ours, have investigated the mechanisms that regulate node of Ranvier formation and maintenance. These studies have shown that node of Ranvier formation and maintenance require myelin

contact. Interestingly, many of the same proteins that cluster at the node of Ranvier also cluster in the AIS; however, the mechanisms responsible for AIS clustering appear to be unique to the AIS as myelin contact is not required and the mechanisms appear to be intrinsic to the neuron. Determining how the AIS is developmentally generated is vital to a complete understanding of the AIS function. However, more in line with understanding the pathobiology of MS, our laboratory is interested in identifying the mechanisms responsible for the maintenance and restoration of AIS integrity and function. To achieve this goal, we have exploited the cuprizone toxicity model. This model results in a consistent course of demyelination followed by remyelination of layer V of the cerebral cortex. Using a combination of immunocytochemistry and confocal microscopy, we have analyzed AIS integrity as evidenced by the clustering of ankyrinG, a prominent initial segment protein. Our findings indicate that the number of AIS is not decreased following myelin loss. In addition, AIS length and surface area are not changed following demyelination. These findings are important as they suggest that myelin is not required for the maintenance of initial segment organization.

.

Introduction

The integrity of the myelin sheath is necessary to maintain normal central nervous system (CNS) function. The maintenance of the CNS myelin sheath is dependent on proper functioning of oligodendrocytes and the viability of the axons they ensheathe (Quarles et al., 2006). Myelin deficiencies may result from a variety of causes, including autoimmunity, viral infections, genetic defects, toxic agents, malnutrition and trauma, which can affect myelin, oligodendrocytes or myelinated neurons (Quarles et al., 2006). A prominent myelin deficient disease affecting more than two million people worldwide is multiple sclerosis (MS) (Dutta and Trapp, 2011). While it is known that axon pathology is a major contributor to impaired motor, sensory and cognitive dysfunction associated with MS (Dutta and Trapp, 2011), the early pathological events responsible for axonal deterioration remain unclear. There are ongoing studies investigating whether axonal pathology associated with MS is a primary consequence of the disease or whether it is a secondary consequence of demyelination. Here, I will investigate the relationship between demyelination and axonal pathology as a secondary event specifically focusing on the AIS.

Myelin

The myelin sheath is an extended plasma membrane that wraps around the neuronal axon and functions in facilitating the conduction of nerve impulses by acting as an insulator. Myelin in the CNS originates from oligodendrocytes (Raine, 1984). An oligodendrocyte extends multiple membranous processes and each process contacts and wraps around a segment of an axon forming a multilayered sheath. The short portions of the axon that are not covered by myelin are called the nodes of Ranvier. The lateral edges of the myelin sheath terminate at the node forming paranodal loops, which participate in the formation of paranodal junctional complexes (Quarles et al., 2006). A structural component of these complexes is transverse bands, which anchor the myelin sheath to the plasma membrane of the axon, or axolemma, (Dupree et al., 1998) and establish and maintain axonal protein domains (Dupree et al., 1999). The segments of myelinated axons between the nodes are known as the internodes (Quarles et al., 2006).

CNS myelin is composed of approximately 30% proteins and 70% lipids. Of the protein component, 60-80% is composed of the myelin proteins, proteolipid protein (PLP) and myelin basic protein (MBP), with the remaining 20-40% being comprised of other minor proteins discussed below (Quarles et al., 2006). PLP makes up greater than 50% of the protein in CNS myelin (Hudson, 2004). The genes of PLP and its alternatively spliced isoform, DM20, are expressed early in development. DM20 mRNA is known to appear even before myelination is initiated. Consistent with a possible role in oligodendrocyte

migration or differentiation (Hudson, 2004), PLP and DM20 are also known to play a role in the stabilization of the intraperiod line (Boison and Stoffel, 1994; Duncan et al., 1987), defined as the apposition of the extracellular surfaces of adjacent layers of the myelin sheath (Fredrik et al., 2011). Although PLP and DM20 serve an important structural and stabilizing role in myelin, the formation of compact, multilamellar myelin is not dependent on them (Coetzee et al., 1999). A *PLP/DM20* knockout mouse initially appeared relatively normal with respect to myelin formation, life span and motor performance (Hudson, 2004). However, the PLP-null mutant is extra sensitive to osmotic shock during fixation, suggesting that PLP may enhance the stability of myelin (Hudson, 2004). In older *PLP/DM20* knockout mice there is significant axonal damage. This suggests that while myelin can form in the absence of PLP/DM20, it is required for the maintenance of axonal structure and function (Hudson, 2004). Interestingly, despite the similarity of PLP and DM20, DM20 cannot replace PLP since the same axonal degeneration was observed in mice only expressing DM20 (Stecca et al., 2000).

MBP comprises 30% of CNS myelin proteins (Liu, 2006). There are four classic isoforms of MBP, whose ratios change with development (Norton and Cammer, 1984). MBP is believed to be the principle protein stabilizing the major dense line of CNS myelin (Quarles et al., 2006). Seven exons of the MBP gene are deleted in the *shiverer* mouse causing a lack of MBP and major dense lines (Gumpel et al., 1983). In the *shiverer* mouse myelin sheaths form, but are severely hypomyelinated and uncompacted suggesting that MBP is necessary for myelin compaction (Gout et al., 1988).

Other proteins present in myelin include 2':3'-cyclic nucleotide 3'-phosphodiesterase (CNP), myelin-associated glycoprotein (MAG) and myelin-oligodendrocyte protein (MOG). CNP is enriched in CNS myelin and oligodendrocytes and is associated with regions of noncompact myelin, such as the oligodendroglial processes and paranodal loops (Quarles et al., 2006; Kursula, 2008). MAG is present in minor concentrations at the periaxonal glial membranes of myelin (Sternberger et al., 1979; Quarles et al., 2006). Not only does MAG's proximity to the axon and its inclusion in the Ig superfamily suggest that it functions in adhesion and signaling between myelin-forming cells and the axolemma (Quarles et al., 1992), but it is also known to bind axonal gangliosides GD1a and GT1b (Schnaar, 2010). It is known that MAG-null mice myelinate relatively normally; therefore, MAG is not essential for myelin formation (Quarles et al., 2006). Unlike MAG, MOG is localized on the outermost surface of myelin sheaths and oligodendrocytes. Similar to MAG, its location suggests that it may function in signal transduction. MOG-null mice exhibit a normal phenotype, leaving its physiological function unclear (Quarles et al., 2006).

Axonal Domains

In addition to providing insulation to the axon, the myelin sheath also serves to divide the axon into molecularly and functionally distinct domains. These distinct domains include the internode, the juxtaparanode, the paranode, the axon initial segment (AIS) and the node of Ranvier (Peles and Salzar, 2000; Salzar, 1997; Arroyo and Scherer, 2000).

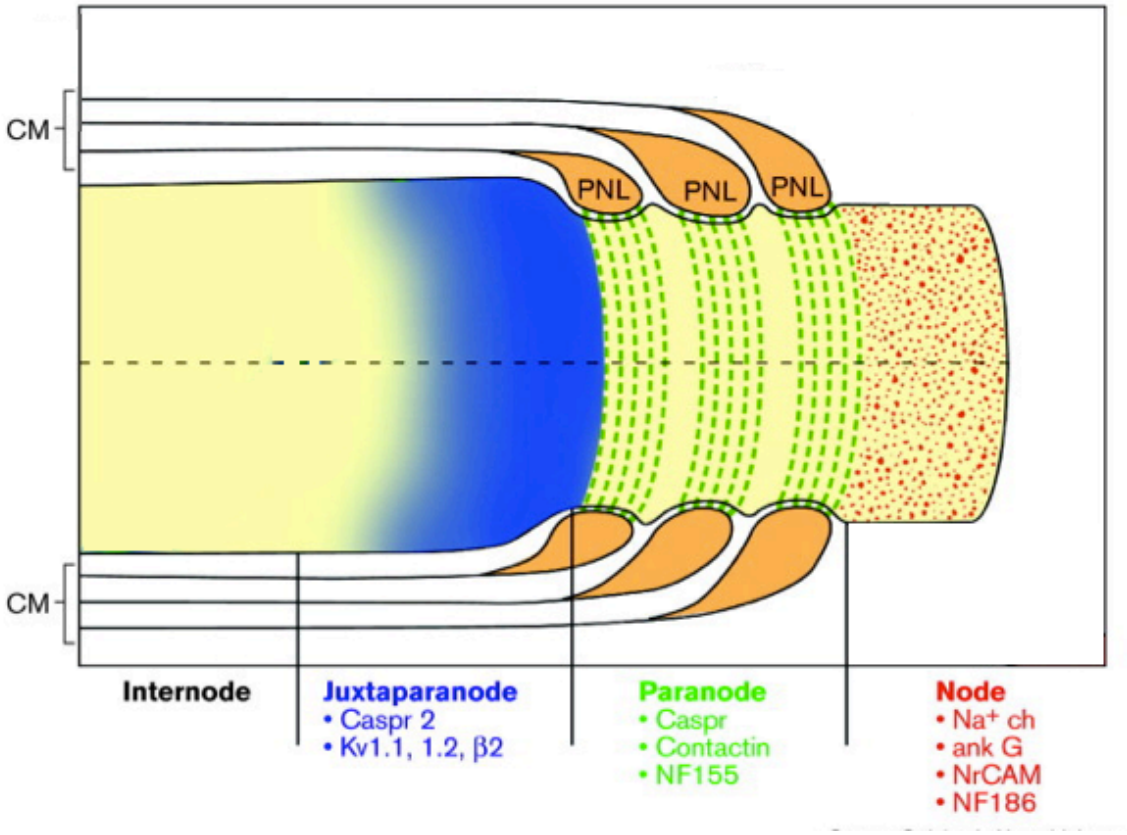

Figure 1. Domains of myelinated axons. An illustration of a longitudinal section through the nodal region of a myelinated axon shows the organization and composition of axon domains in relation to the myelin sheath. Beneath the compact myelin (CM) is the internode, which is adjacent to the juxtaparanode. K^+ channels and caspr2 are concentrated at juxtaparanodal regions. The CM sheath opens into a series of perinodal cytoplasmic loops (PNL) at the paranode. Paranodal proteins include caspr, contactin and neurofascin-155. The node of Ranvier lacks myelin and contains Na^+ channels, ankyrinG, NrCAM and neurofascin-186. (Adapted from Peles and Salzar, 2000).

The internode is the region of the axon covered by the compact myelin sheath. It is the longest segment of the myelinated axon (Trapp and Kidd 2004). There are no known proteins specifically enriched in the CNS internode (Peles and Salzar, 2000). Additionally, the molecules that maintain myelin-axon adhesion remain unknown. However, dual elimination of MAG and myelin galactolipids result in internodal myelin deterioration suggesting possible roles in adhesion (Marcus et al., 2002).

Juxtaparanodes comprise the region of axon covered by compact myelin (Peles and Salzar, 2000). The juxtaparanode may be considered a specialized portion of the internode containing the K^+ channels $K_v1.1$, $K_v1.2$ and their $K_v\beta2$ subunit. These channels are important in maintaining the internodal resting potential by quickly repolarizing the axon following an action potential (Wang et al., 1993; Rasband et al., 1998; Vabnick et al., 1999). Associating with these K^+ channels is the protein, caspr2 (contactin-associated protein 2) (Poliak et al., 1999), forming a complex with transient axonal glycoprotein-1 (TAG-1) (Traka et al., 2003). This interaction with TAG-1 provides anchorage between the myelin sheath and axon (Wang et al., 1993).

Compact myelin lamellae open into a series of loops that spiral around and closely appose the axon on either side of the node of Ranvier at paranodal junctions. Paranodes are located adjacent to juxtaparanode and are important in anchoring the myelin loops to the axon (Rosenbluth, 1995). The axo-glial junctions found at the paranode include two axonal membrane proteins known as contactin and caspr (contactin-associated protein) (Peles et

al., 1997). Caspr and contactin form a *cis* complex (Tait et al., 2000) that binds to the oligodendrocyte protein neurofascin-155 (NF-155) (Davis et al., 1996). Together these proteins form an axo-glial complex with caspr serving as the transmembrane scaffold that stabilizes the complex with cytoskeletal anchors (Gollan et al., 2002).

The AIS is the unmyelinated region of the axon just distal to the cell body, which is responsible for the initiation, modulation and propagation of action potentials (Buffington and Rasband, 2011). In the AIS there is an enrichment of voltage-gated Na^+ channels, most popularly Na_v 1.6 (Caldwell, et al., 2000), but also Na_v 1.2 and Na_v 1.1 (Buffington and Rasband, 2011). These channels are responsible for inward current flow and control action potential initiation and propagation (Peles and Salzar, 2000; Buffington and Rasband, 2011). Binding to and anchoring voltage-gated Na^+ channels is the cytoskeletal scaffolding protein, ankyrinG (ankG) (Buffington and Rasband, 2011). AnkG colocalizes with the actin-binding protein, βIV spectrin, and anchors the neural cell adhesion molecule (NrCAM) and neurofascin186 (NF-186) to the axon (Kordeli et al., 1990; Berghs et al., 2000). These axo-glial interactions are essential for proper functioning of the axon.

Similar to the AIS, another area of the axon lacking myelin is the node of Ranvier. The node is important in propagating the action potential initiated at the AIS. Interestingly, both the AIS and node have a similar protein composition. At the node there is also an enrichment of voltage-gated Na^+ channels (Peles and Salzar, 2000; Buffington and Rasband, 2011), which are anchored by ankG (Buffington and Rasband, 2011). In the node

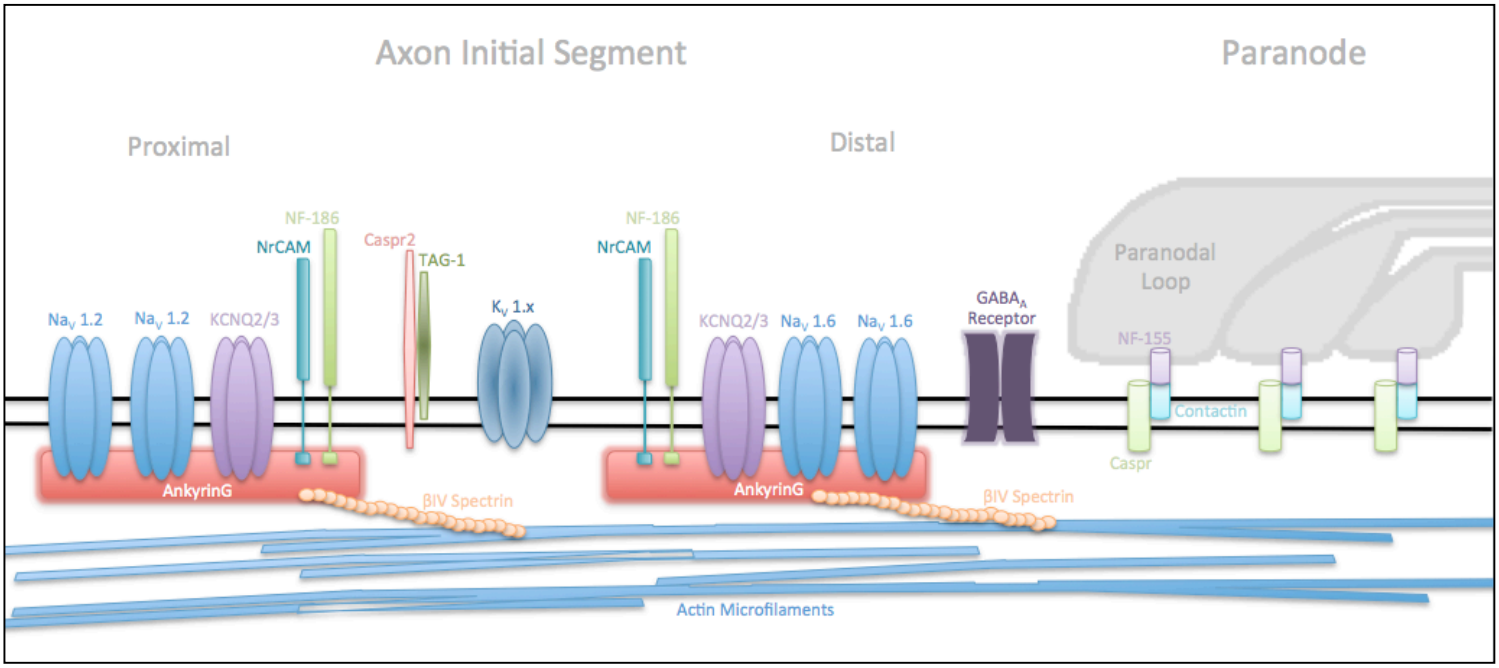

Figure 2. Axon Initial Segment and Paranodal Proteins. Ion channels, cell adhesion molecules, neurotransmitter receptors and cytoskeletal proteins are enriched at the AIS. Na_v 1.2 channels are clustered at more proximal regions of the AIS, while Na_v 1.6 channels are found at distal regions. Similarly $GABA_A$ receptors are only found at distal AIS. At the paranode caspr and contactin are bound in *cis.* They form a complex with the glial protein, neurofascin-155.

ankG colocalizes with βIV spectrin and interacts with NrCAM and NF-186, as well (Peles and Salzar, 2000; Buffington and Rasband, 2011).

Formation of Nodes of Ranvier

Studies have shown the importance of myelin for the formation of nodal clustering. Using lysolecithin to induce demyelination, Dugandžija-Novaković et al. (1995) first reported that nodal Na^+ channel clustering was dependent on myelination. In this study, the authors reported that Na^+ channel clustering only occurred in the areas of remyelination. Following the injection of the demyelinating agent, Na^+ channel clustering was only seen at heminodes, which marked the transition from myelinated to demyelinated regions at the edge of the injected zone, and at widely spaced sites that were thought to be former nodes. As the myelinating Schwann cells proliferated and repopulated the demyelinated region, myelin forming processes adhered to axonal internodes and as the myelinating processes advanced along the axon, Na^+ channel clusters appeared at the borders of these processes. As the Schwann cell processes continued to advance along the unmyelinated axon, the clusters remained at the edges and moved with the process as it elongated during remyelination. As the remyelinating process continued, the Na^+ channel cluster at the edge of one process approached the cluster at the edge of an adjacent process eventually forming a new node.

Vabnick and Shrager (1998) further looked into myelin's role in Na^+ channel clustering during development. They observed that it is only after the expression of myelin-associated glycoprotein (MAG), a myelin-forming cell protein that is expressed after the cell has an overlapping ensheathement and is committed to myelination (Martini and Schachner, 1986), that the frequency of occurrence of Na^+ channel clusters rises sharply. Together, with the previous work of Dugandžija-Novaković et al. (1995), these findings suggests that not only does myelin mediate formation of Na^+ channel clusters in the PNS, but there must also be close axon-glial contact for the initiation of nodal clusters (Vabnick and Shrager, 1998).

Using mice that lack galactose-ceramide galactosyltransferase (CGT), an enzyme needed for the production of the myelin components, galactocerebroside (GalC) and sulfatide (Morell and Radin, 1969), Dupree et al. (1999) showed the importance of axo-glial interactions in the molecular organization of the nodal region of the CNS. In the spinal cords of CGT knock outs, nodal and paranodal abnormalities were observed including altered node length, terminal loops that frequently face away from the axon and a complete absence of transverse bands, which are prominent components of the paranodal septate-junctions (Dupree et al., 1998 and Popko, 2000). This severe alteration in axo-glial interactions resulted in abnormal ion channeling clustering with elongated nodal Na^+ channel clusters and failure of K^+ channel clustering at the juxtaparanode (Dupree et al., 1999).

Although these early studies demonstrated the importance of the myelin sheath and its proper adhesion to the axon in the regulation of the ion channel clustering, these studies did not identify the molecules that mediate domain formation. More recently, Peles and colleagues reported that initial step in Na^+ channel clustering in the PNS involves the Schwann cell protein gliomedin (Eshed et al., 2005). As shown by Bhat (Thaxton and Bhat, 2009) and others (Labasque et al., 2011), gliomedin binds the extracellular domain of the neuronal nodal protein, neurofascin186 (NF-186), which initiates the recruitment of other nodal proteins (Lambert et al., 1997; Eshed et al., 2005; Schafer et al., 2006; Feinberg et al., 2010). After NF-186 is localized to the node, it recruits ankG to the node through its FIGQY binding motif (Dzhashiashvili et al., 2007). Na_v channels then bind to ankG (Rasband, 2008). AnkG also interacts with the neuronal cytoskeleton through its interaction with βIV spectrin (Berghs et al., 2000), an actin binding protein that serves to link nodal proteins to the neuronal cytoskeleton (Buffington and Rasband, 2011).

The formation of CNS nodes is not as well understood. One hypothesis suggests that a possible candidate for a CNS equivalent to gliomedin is the extracellular matrix (ECM) protein, brevican, which is known to localize to the node (Bekku et al, 2009). However, ablation of *brevican* in mice revealed no major defects in nodal organization (Brakebush et al., 2002), but it may be possible that other proteins function together with brevican to organize the node and compensate in the brevican knockout mice (Buttermore et al., 2013). Therefore, the protein that initiates CNS nodal ion channel clustering remains unclear.

Although conflicting, other work has proposed that oligodendrocytes have the ability to induce Na^+ channel clustering through secretion of soluble factors independent of myelin contact (Kaplan et al., 1997). However, further examination revealed that in the oligodendrocyte conditioned medium only Na_v 1.2 channels, the immature Na_v channel isoform, clustered at the node. Subsequent work by Kaplan et al. (2001) revealed that myelination is required for the clustering of Na_v 1.6 channels, the mature nodal isoform, at the nodes. Although the role of a soluble factor has not been disproved, at least for the clustering of the immature form of Na^+ channels, overwhelming evidence indicates that myelin sheath formation is required for CNS nodal clustering. Using a mouse that exhibits severe hypomyelination of the CNS, Rasband et al. (1999) demonstrated that CNS nodal clustering required myelin-axon contact. Moreover, nodal clustering of ankyrinG was also shown to be dependent on axo-glial contact.

Formation of AIS

Unlike the node, formation of the AIS does not require myelin and occurs intrinsically though the localization of ankG (Bennett and Baines, 2001). Although the signals responsible for ankG localization to the AIS are still unknown, it is known that ankG is a cytoskeletal scaffolding protein that functions to stabilize proteins by linking them to the actin-spectrin cytoskeleton (Bennett and Lambert, 1999). More specifically, following ankG localization to the AIS it then recruits βIV spectrin (Yang et al., 2007). It is through ankG interaction with βIV spectrin that it associates with the actin cytoskeletal network

(Buffington and Rasband, 2011). Recent work has shown that Na_v 1.6 channels' ankG-binding domain is required for their localization at the AIS (Gasser et al., 2012). The importance of ankG in AIS formation is shown in studies using ankG knockouts and knockdowns since genetic ablation of ankG results in failure of NF-186 and ion channel clustering at the AIS (Zhou et al, 1998; Hedstrom et al., 2007).

While ankG is necessary for initial AIS organization, recent work has shown that NF-186 is needed for AIS maturation (Buttermore et al., 2012). A critical step in the maturation process of the AIS is the switch in the expression of Na_v 1.2 channels to the expression of Na_v 1.6. (Boiko et al., 2003; Van Wart and Matthews, 2006). A similar switch is expression also occurs at the node (Boiko et al., 2001); however, at the node a complete switch occurs. In contrast, at the AIS, Na_v 1.2 remains but is restricted to the proximal portion of the AIS while Na_v 1.6 clusters at the distal region of the AIS. (Hu et al., 2009). In the absence of NF-186, mature Na_v 1.6 channels are not enriched at the AIS and the Na_v 1.2 channels persist (Buttermore et al., 2012). This suggests that initial clustering mechanisms are distinct from those that regulate maturation and perhaps maintenance.

Maintenance of Nodes of Ranvier

In addition to playing a critical role in initiating Na^+ channel clustering, the myelin sheath also is essential for maintaining the clustering of these ion channels. The previously mentioned work performed by Dugandžija-Novaković et al. (1995) also highlights the

importance of myelin in the maintenance of Na^+ channel clusters. Following lysolecithin injection, myelin is completely void from the focal area after one week coinciding with the loss of Na^+ channel clusters (Dugandžija-Novaković et al. 1995). For example, using a conditional knockout approach, Pillai et al. (2009) generated a mouse that lost expression of NF-155, the glial-specific neurofascin expressed at the paranode, after initial Na^+ channel clustering occurred. These mice exhibited disassembly and distal unraveling of axo-glial junctions from the juxtaparanode towards the node. Although the node initially remained intact, with extended time NF-186, Na_v channels and ankG diffused out indicating that the long-term integrity of the node relies on myelin-axon contact (Thaxton and Bhat, 2009).

Studies have also examined the role of nodal proteins in the organization and stabilization of CNS nodes. Deficiencies in βIV spectrin resulted in altered axonal shape (Yang et al., 2004) and decreased levels of ankG and Na_v channels at nodes suggesting its role in node stabilization (Komada and Soriano, 2002; Lacas-Gervias et al., 2004). Mice that lacked both NF-186 and NF-155 exhibited a complete disorganization of both the paranode and node (Sherman et al., 2005) while absence of only NF-186 resulted in the invasion of paranodal proteins into the nodal gap (Thaxton et al., 2011).

Maintenance of AIS

AnkG is not only essential for AIS assembly (Hedstrom et al., 2007), but is also required for AIS maintenance (Hedstrom et al., 2008). Using gene silencing mechanisms, it has been shown that loss of ankG from the AIS results in a disassembling of AIS protein clusters (Hedstrom et al., 2008). In this study neurons lacking ankG also had a decrease in Na_v channels, βIV spectrin, NF-186 and NrCAM, a neuronal cell adhesion molecule (Thaxton and Bhat 2009). Therefore ankG is not only necessary for the initial recruitment of these protein clusters to the AIS, but also their long-term stability (Hedstrom et al., 2008). These artificial conditions have shown the importance of ankG in AIS maintenance, but no study has investigated myelin's role in maintaining the AIS. This is an important question since the loss of myelin is known to contribute to axonal pathology in disease, such as multiple sclerosis.

Multiple Sclerosis

Multiple sclerosis (MS) is the leading cause of non-traumatic neurological disability in young adults in the United States and Europe (Dutta and Trapp, 2011). MS is a disease affecting the CNS that involves both inflammation and widespread myelin loss. MS is diagnosed by the presence of multifocal inflammatory demyelinated plaques within the CNS. In addition to demyelination and multifocal inflammation, other pathologies associated with MS include the breakdown of the blood-brain barrier (BBB) and reactive

gliosis. However, the primary pathology of MS is characterized by an immune-mediated destruction of myelin and oligodendrocytes in the CNS, but studies have shown that progressive axonal loss is the major cause of irreversible neurological disability in MS (Stadelmann et al., 2008; Trapp and Nave, 2008).

MS Inflammation

While the CNS has few lymphocytes present in the absence of infection, a small population of lymphocytes provides surveillance for infection or injury and is part of a healthy immune system (Hickey et al, 1991; Wekerle et al., 1987). Moreover, these lymphocytes may also provide important inflammatory signals needed for wound healing, angiogenesis and neuroprotection (Hauser and Oksenberg, 2006). However, the transition from healthy to pathological autoimmunity can occur. T cells activated in the periphery cross the BBB and enter the CNS (Hauser and Oksenberg, 2006; Hickey et al., 1991; Wekerle et al., 1987). Activation of autoimmune responses against myelin components in the CNS is hypothesized to occur through a variety of mechanisms such as molecular mimicry, bystander activation and epitope spreading (Vanderlugt and Miller, 2002; von Herrath et al., 2003). Once activated, myelin-specific T cells can cross the BBB where they proliferate and secrete pro-inflammatory cytokines, such as TNF- α (Peterson and Fujinami, 2007). These cytokines stimulate microglia, macrophages and astrocytes, and recruit B cells, which ultimately results in damage to myelin, oligodendrocytes and axons (Zamvil and Steinman, 2003).

MS Demyelination

Demyelination associated with "MS lesions," the breakdown of the BBB, infiltration of lymphocytes, demyelination and oligodendrocyte death, occurs throughout the CNS (Dutta and Trapp, 2011). While MS was initially regarded as a white matter disease, with an autoimmune response against myelin, the involvement of grey matter is becoming more evident. As is the case in white matter, axons in the grey matter are myelinated, and demyelination of axons in grey cortical matter regions has been reported as a prominent feature on post-mortem examination of patients with MS (Bo et al., 2003).

Axonal Pathology Associated with MS

Axonal loss could be a result of nonspecific damage caused by inflammation (Trapp et al, 1998; Dutta and Trapp, 2010). During the inflammatory process activated immune and glial cells release many substances including proteolytic enzymes, cytokines, oxidative products and free radicals that can damage axons (Hohlfeld, 1997). Inflammation also affects energy metabolism, ATP synthesis and mitochondrial DNA and impairs the mitochondrial enzyme complexes (Lu et al., 2000; Dutta et al., 2006) While the mechanisms of axon loss are unknown, there is a strong correlation between inflammation and axon transection suggesting that immune-mediated mechanisms may contribute to axonal pathology in MS (Dutta and Trapp, 2010). However, studies have shown that axon injury and loss are also evident in chronically demyelinated lesions where little or no

active inflammation was observed. This would suggest that myelin plays an important role in maintaining axon integrity. More specifically, myelin is known to be important in the maintenance of axonal domains ((Dupree et al., 1999; Dupree et al., 2004; Marcus et al., 2006; Pomicter et al., 2010), which is essential for proper axonal function.

Myelin is Required for the Maintenance of Axonal Domains

It is recognized that maintaining proper axonal function is intimately related to proper establishment and maintenance of axonal domains such as the node of Ranvier and the AIS (Bhat et al, 2001; Buttermore et al., 2013). Previous studies in our lab have determined that myelin contact is required for node of Ranvier formation and maintenance (Dupree et al., 1999; Dupree et al., 2004; Marcus et al., 2006; Pomicter et al., 2010). While the node of Ranvier and AIS cluster many of the same proteins (Buffington and Rasband, 2011), the mechanisms responsible for initial AIS protein clustering appear to be unique since myelin contact is not required (Zonta et al., 2011). Although studies have investigated the mechanisms that initiate protein clustering at the AIS (Hedstrom et al., 2007), there are no studies that have addressed the maintenance of these axonal domains. Here, we address this void in our understanding by testing the hypothesis that myelin is required to maintain AIS protein clusters.

Models of Demyelination

To investigate the role that myelin plays in the maintenance of protein clusters within the AIS, we needed to choose the most appropriate model of CNS demyelination and remyelination. The ideal model would generate a highly reproducible lesion of the grey matter, specifically target oligodendrocytes, and exhibit minimal general toxicity and inflammatory responses. Within the myelin literature, several models have been characterized including Theiler's Murine Encephalomyelitis Virus (TMEV), lysolecithin and cuprizone. TMEV is single stranded RNA virus that belongs to the family *Picornaviridae* (Roos et al., 1992). It is classified among a subgroup of cardioviruses (Pevear et al., 1987) and is a natural pathogen for mice (Roos et al., 1992). In the wild the virus causes an infection of the enteric tract and may occasionally become paralytic (Dal Canto et al., 1995). TMEV is one of the first viruses able to produce chronic infection, which is important for studying demyelination (Dal Canto et al., 1980). *It* is divided into two subgroups, GDVII and Theiler's original (TO), based on its neurovirulence in mice. The GDVII subgroup is highly virulent producing encephalitis and death in less than a week in most animals (Dal Canto et al., 1995). The TO subgroup produces a chronic persistent CNS infection, which results in inflammatory demyelination (Dal Canto et al., 1980). However, there is a spectrum of susceptibility to TMEV-induced demyelination among mouse strains (Dal Canto et al., 1980).

Lysolecithin is a lipid with detergent-like properties. It is thought to cause demyelination by acting as a membrane-solubilizing agent with a particular toxicity to myelinating cells (Woodruff and Franklin, 1999). Lysolecithin causes CNS demyelination when focally injected in vivo into specific myelinated fiber tracts (Birgbauer et al., 2004). Demyelination is observed within 30 minutes of lysolecithin injection; however, there is an accumulation of dense bodies and degenerating mitochondria (Hall, 1972). Lysolecithin allows for the study of remyelination since remyelination is observed within 14 days following injection (Hall, 1972). While this model provides consistent demyelination and remyelination, specificity of target remains unclear.

Exposure of the neurotoxicant, cuprizone (bis-cyclohexanone-oxaldihydrazone), to young adult C57BL/6 mice induces a synchronous and consistent model for demyelination followed by remyelination (Mason et al., 2001; Matsushima and Morell, 2001; Skripuletz et al., 2008). Demyelination occurs at sites large enough to allow detectable cellular, molecular, biochemical and morphological changes (Matsushima and Morell, 2001). Removal of cuprizone from the diet allows for the study of remyelination (Matsushima and Morell, 2001). Previous work (Skripuletz et al., 2008) has shown that cortical demyelination and remyelination is prominent in the cuprizone model. Although cuprizone is a toxin, titrating it down to 0.2% allows for demyelination with minimal toxic effects (Matsushima and Morell, 2001).

Although the exact mechanism of the cuprizone model of demyelination is unknown, cuprizone is known to be a copper chelator. The feeding of cuprizone is thought to induce a copper deficiency (Suzuki and Kikkawa, 1969; Kesterson and Carlton, 1971; Pattison and Jebbett, 1971; Blakemore, 1972; Blakemore, 1973; Ludwin, 1978), which is thought to be detrimental to mitochondrial function (Venturini, 1973) and that it is a disturbance of energy metabolism in the oligodendrocytes and cell function that leads to demyelination (Cammer and Zhang, 1993; Fujita et al, 1993; Komoly et al., 1987; Morell et al., 1998). This demyelination can be detected early without damaging cell types other than oligodendrocytes (Blakemore, 1973; Cammer and Zhang, 1993; Fujita et al., 1990; Komoly et al., 1987; Ludwin, 1978). The hypothesis as to why oligodendrocytes are preferentially susceptible to the copper deficit is that these cells must maintain a great amount of myelin and this great metabolic demand places it at risk if the demand is not met (Matsushima and Morell, 2001).

While axonal pathology contributes to much of the dysfunction associated with MS (Dutta and Trapp, 2011), the early pathologic events responsible for axonal deterioration remain unclear. In this study we have chosen to exploit the cuprizone toxicity model to address whether the maintenance of the AIS integrity is dependent on the presence of an intact myelin sheath because this model not only provides limited off target toxicity, is easy to administer but also provides a consistent course of demyelination followed by remyelination of the 5th layer of the cerebral cortex (Skripuletz et al., 2008). Together, these features make cuprizone the ideal model to test our hypothesis that the maintenance

of the AIS of myelinated axons requires myelin-axon interactions and that re-establishment of these interactions initiates the restoration of AIS integrity.

Materials and Methods

Animals

Five week old male C57/black6 mice were purchased from the Jackson Laboratory (Bar Harbor, ME) and maintained in the Virginia Commonwealth University Division of Animal Resources vivarium, which is an AAALAC accredited facility. Treatment was initiated after allowing the mice to acclimate for one week. Food and water were provided *ad liberatum*. All procedures were conducted in accordance to the methods outlined in the approved IACUC protocol AD20186.

Ground rodent chow (5001 Rodent Diet; PMI Nutrition International, LLC, Brentwood, MO) was mixed with cuprizone (Bis-cyclohexanone oxaldihydrazone; Sigma-Aldrich, St. Louis, MO) and vigorously shaken for 5 minutes following a previously described protocol (Hiremath et al., 1998; Dupree et al., 2004). Treated animals were removed from cuprizone after either 3 or 5 weeks of treatment and were immediately processed for tissue analysis. An additional group was maintained on cuprizone for 5 weeks followed by an additional 3 weeks on normal (non-cuprizone) chow. Three weeks of normal chow has been previously shown to maximize myelin repair. (See Table I for treatment dose and duration and for the number of mice analyzed in each treatment group).

	3 weeks	5 weeks	5+3 weeks
0% Cuprizone	3	3	3
0.2% Cuprizone	3	4	4

Table I. Cuprizone dose and duration. A minimum of 3 mice were maintained on a ground chow diet either without (0% cuprizone) or with (0.2% cuprizone) for 3 or 5 weeks. These durations were chosen based on previous studies that have reported that the initial signs of demyelination occur following 3.5 weeks of exposure and maximum demyelination occurs after 5 weeks of exposure. An additional group of mice were maintained for an addition 3 weeks on non-cuprizone containing ground chow to facilitate remyelination.

Tissue Preparation

Anesthesia

After the appropriate treatment times, mice were deeply anesthetized using 0.016 mL/gm body weight of a 2.5% solution of avertin (2, 2, 2 tribromoethanol) (Sigma-Aldrich; St. Louis, MO) in 0.9% sodium chloride (NaCl) (Sigma-Aldrich). The working dilution of 2.5% avertin was generated from a stock solution of 100% avertin which was dissolved in tert-amyl alcohol (Acros Organics, NJ) and stored at 4°C. The appropriate volume of avertin was injected intraperitoneally using a 27 gauge, ½ inch long needle attached to a 1 milliliter syringe (Becton, Dickinson & Company, Franklin Lakes, NJ). Following injection the mouse was returned to its cage to allow for the anesthesia to take effect. Consciousness was checked using a combination of a toe pinch and corneal reflex.

Perfusion

After anesthesia the mouse was stabilized ventral side up on a dissecting block. An initial incision was made from the abdomen to the sternum and two more incisions were made from the sternum to each axilla resulting in a 'Y' shaped incision. To expose the heart the diaphragm was severed and the rib cage was excised. A cut was made in the right atrium to allow for an exit point for the blood and perfusate. A 22 gauge 1 inch needle was then inserted into the left ventricle making sure not to puncture the interventricular septum or the aorta.

Following a 0.9% NaCl flush for 5-7 minutes or until the perfusate flowed clear, the mouse was transcardially perfused with freshly prepared phosphate buffer containing 4% paraformaldehyde (Electron Microscopy Services, Hatfield, PA). After muscle twitching stopped, the fixative solution was continued for 10 minutes, at a rate of 7 milliliters per minute, to allow for a mild fixation, which is beneficial for immunocytochemical labeling. The entire brain, with the exception of the olfactory bulbs, was immediately harvested and placed in phosphate buffered saline (PBS) (137 mM NaCl, 10 mM Na_2HPO_4, 1.8 mM KH_2PO_4, 2.7 KCl, with a pH of 7.4) containing 30% sucrose. Following 48 hours of incubation in the PBS-containing sucrose, the brains were frozen in Optimal Cutting Temperature (OCT), sectioned at 10 μm using a Leica CM 1850 cryostat. Previous work (Skripuletz et al., 2008) observed consistent cortical demyelination in regions spanning between bregma -0.94 and bregma -1.8. Based on this previous work, 15 sets of six 10 μm sections harvested from cortical regions, approximately 90 um apart, were collected. Slides were labeled with cuprizone treatment and mouse number. Each set of 6 sections were placed on ProbeOn Plus slides (Fisher) and stored at -80°C until they were immunolabeled.

Immunocytochemistry

Slides were randomly selected and removed from the -80°C freezer and allowed to dry before cutting away excess OCT from the perimeter. Using a PAP pen (Super PAP Pen, Electron Microscopy Sciences), a hydrophobic barrier was drawn around the tissue to maintain solutions on the slide. Slides were then placed in -20°C acetone and allowed to permeabilize for 10 minutes. The slides then underwent three 5 minute rinses in PBS

followed by a 15 minute incubation in blocking solution. The blocking solution contained ~5% cold water fish gelatin and 0.1% Triton X-100 in PBS. The exception to this general protocol was with labeling for the myelin protein myelin basic protein (MBP). MBP is a cytoplasm protein that is more difficult to immune-label and additional permeabilization is required. Therefore, when using the MBP antibody, 1% Triton X-100 was used in place of the 0.1% Triton X-100 concentration stated above. After slides were removed from the blocking solution, they were incubated in the appropriate primary antibody at the concentration shown in Table II.

Primary Antibody	AnkyrinG (ankG) (NeuroMab)	Dephosphorylated Neurofilament (SMI 32) (Covance)	Myelin Basic Protein (MBP) (Sternberger Monoclonal)	Caspr (gift from Dr. Manzoor Bhat)	Amyloid Precursor Protein (APP) (Invitrogen)	Neuronal Nuclei (NeuN) (Millipore)
Dilution	1:200	1:1000	1:1000	1:1000	1:500	1:1000
Secondary Antibody (1:500)	Alexa 594 Anti-Mouse IgG2a	Alexa 594 Anti-Mouse IgG1	Alexa 488 Anti-Mouse IgG2b	Alexa 488 Anti-Guinea Pig IgG	Alexa 488 Anti-rabbit IgG	Alexa 594 Anti-Mouse IgG1

Table II. Primary and Secondary Antibody Concentrations

The tissue was incubated overnight at 4°C in the primary antibody in a humidified chamber to prevent drying. The next day three PBS rinses and the 15 minute blocking steps were repeated. The slides were then incubated for 90 minutes in secondary antibody (Table II), which were fluorescently conjugated and diluted to a 1:500 concentration in the blocking solution, in a light tight, humidified chamber at room temperature. After removal of the secondary antibody, the slides were dipped once in PBS to remove the secondary antibody followed by three additional 5 minute rinses. They were then incubated in the nuclear label bisBenzamide at a concentration of 1:1000 for 5 minutes. The slides were then exposed to three 5 minute rinses in PBS and then mounted with Vectashield™ (Vector Laboratories) medium, cover slipped and imaged.

Image Collection

Confocal Microscopy

All sections were imaged using a Zeiss LSM 700 confocal laser scanning microscope (Carl Zeiss Microscopy, LLC, Thornwood, NY), which is housed in the VCU Department of Anatomy and Neurobiology Microscopy Facility. Sixteen fields were collected per mouse. All images were collected from cortical layer V, since this region is not only clearly identifiable with a bisBenzamide stain (Figure 2), but also contains a relative homogenous neuronal population with approximately 80% cortical Pyramidal neurons and 20% interneurons. Right or left hemisphere was randomly chosen and two fields from both medial and lateral aspects were sampled. The longitudinal fissure was used to identify the

midline of the brain. Adjacent to the longitudinal fissure, AIS are oriented in an oblique direction and the delineation of the cortical layers is less clearly demarcated. In order to ensure comparison of comparable cortical regions, 2 medial images were collected just lateral to the region of the obliquely oriented AIS.

At the lateral extent of the cortical regions, the cortical layers bend to accommodate the curvature of the ventral aspect of the brain. Similar to the cortical regions adjacent to the longitudinal fissure, the AIS in these most lateral extents are also obliquely oriented. Therefore, the two lateral images were collected from the regions where the AIS were obliquely oriented. In these regions cortical layer 5 was easily and reproducibly identified. In all cases a z-stack of 14 optical planes was collected using Nyquist sampling, which was calculated at a step size of 0.51 μm. Gain and offset were held between 680-710, using fluorescent beads as a standard and adjusting gain and offset settings to the same intensity. Table III contains a list of settings used for image collection. All image analyses were conducted under the supervision of Dr. Scott Henderson, Director of the VCU Microscopy Facility.

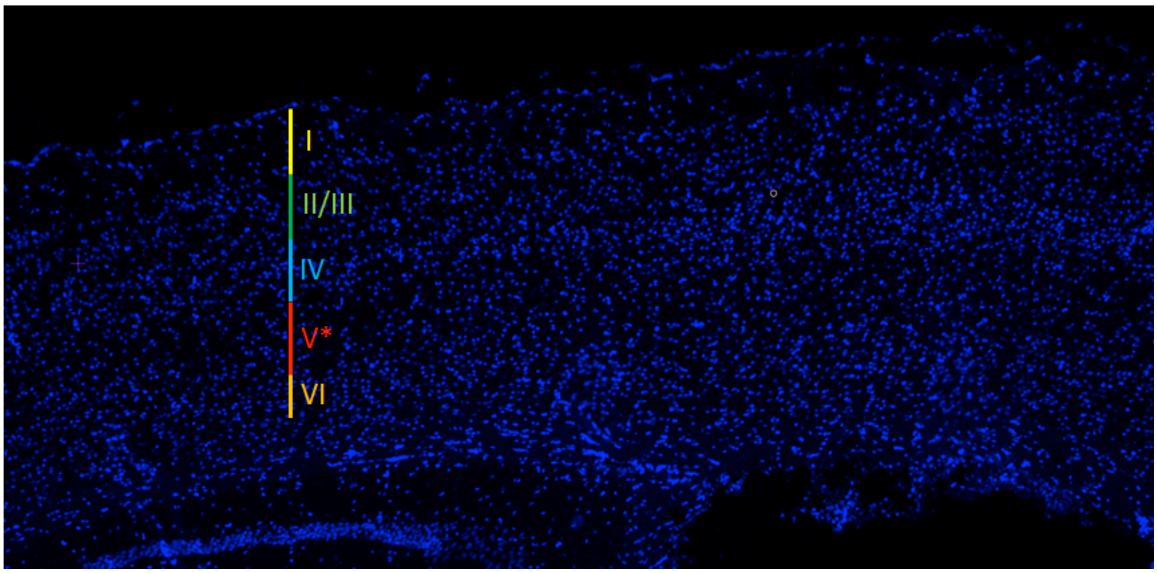

Figure 2. bisBenzamide labeling demarcating cortical layers. Cortical layer V, a region populated by approximately 80% pyramidal neurons, demyelinates following cuprizone treatment. Thus, providing an ideal model for initial segment analysis. (bisBenzamide-blue)

Gain	Offset	Pinhole	Zoom	Objective	Format	Line Average	Pixel Size	Step Size
680-710	0	1 Airy Unit	1	40x	1396 x 1396	2	0.11 μm	0.51 μm

Table III. Confocal Microscope Settings

Analysis

Using the image analysis software Volocity™ (Perkin-Elmer, Waltham, MA), which is housed in the VCU Department of Anatomy and Neurobiology Image Analysis Facility, the number, surface area and length of initial segments were determined.. Optimal data collection parameters were determined based on the recommendations of Dr. Scott Henderson. For every z-stack analyzed the minimal threshold was determined by checking maximum intensity of objects that were certain to not be initial segments and identifying the minimum pixel intensity of objects that were identified as AIS. Although these minimum intensities varied from image to image, the variability was slight ranging between 210 and 400**.** Because AIS are more elliptical, shape was used to exclude nodes of Ranvier and lipofuscin, which is a build-up of strongly oxidized proteins and lipids known to accumulate in stressed or aged cells (Jung et al., 2007). More spherical objects were excluded by only collecting objects that had a minimum shape factor of 0.4. To further ensure that nodes of Ranvier were not mistakenly analyzed, collected objects less than 15 μm^3, which is consistent with the area of a node but dramatically smaller than AIS, were excluded. ImageJ (NIH) was also used to analyze length and number of initial segments. All AIS counts, indicating the numbers of AIS analyzed were presented as actual values (mean +/- SEM). AIS surface area and length data collected using Volocity™ are presented as percent of the mean +/- percent of SEM while length values collected using ImageJ are presented as actual value means +/- SEM. All data were statistically analyzed using a t-test comparing untreated to 3 weeks treated, untreated to 5 weeks treated or untreated against 5 weeks treated followed by 3 weeks of myelin repair.

Results

Cortical layer V demyelinates following cuprizone treatment

In order to initiate cortical demyelination followed by remyelination, cuprizone was administered at a 0.2% concentration consistent with the treatment paradigm used by Skripuletz et al. (2008). Immunolabeling for myelin basic protein (MBP) provided a qualitative assessment of the extent of myelin loss in the cortical layer V of mice maintained on ground chow containing 0.2% cuprizone. As shown in Figure 3A, robust MBP labeling was observed in mice maintained on ground chow without cuprizone. In contrast, as early as 3 weeks of cuprizone treatment, a reduction in the level of MBP labeling was consistently observed in cortical layer V (Figure 3B). Interestingly, cortical demyelination was not observed by Skripuletz et al. (2008) following only 3 weeks of cuprizone exposure. Following 5 weeks of treatment, an exposure duration that has previously been reported to elicit maximum CNS demyelination (Matsushima and Morell, 2001), MBP labeling revealed a continued, progression of myelin loss throughout all cortical layers (Figure 3C). Importantly, maintaining the mice for an additional 3 weeks on ground chow without cuprizone resulted in an increase in MBP labeling, which is consistent with remyelination of cortical layer V (Figure 3D). Together, this qualitative assessment confirmed the temporal course of demyelination/remyelination induced by

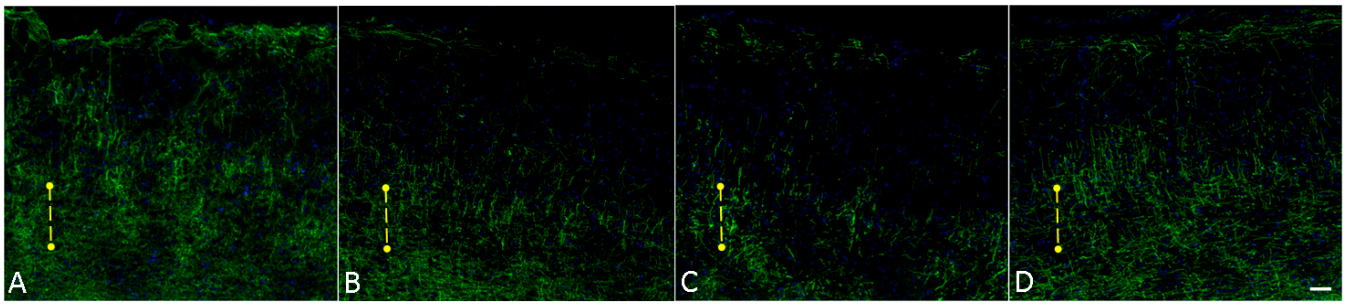

Figure 3. Cortical layer V demyelinates following cuprizone treatment. Immunolabeling of myelin basic protein (green), a prominent protein of the myelin sheath, was used to assess control levels of myelin (A, no cuprizone treatment), and the extent of demyelination (B, 3 week treated; C, 5 week treated) and remyelination (D, 5 weeks treated, 3 weeks recovery). The yellow dashed line indicates the approximate level of cortical layer V. Scale bar: 40 μm

cuprizone exposure and cuprizone withdrawal. Moreover, it illustrates that the mice used for our analyses of the AIS also exhibited a similar profile of myelin damage and repair.

Cell death was not observed among treatments

As the above qualitative assessment revealed that the cuprizone toxicity model was successful in inducing demyelination and remyelination in the cerebral cortex, we wanted to determine whether this loss of myelin resulted from neuronal death. Previous work from our laboratory (Dupree et al., 2004) and others (Matsushima and Morell, 2001) has shown that cuprizone demyelination results from oligodendrocyte death; however, demyelination might also be a consequence of neuronal death. Since the basis of my study was to assess AIS changes induced by demyelination as the primary insult, assessment of neuronal and axonal health is critical. The first approach in assessing neuronal health was to determine whether cuprizone treatment resulted in neuronal loss in cortical layer V. To assess the neuronal population of cortical layer V, sections were immunolabeled with an antibody directed against NeuN, a neuronal specific marker (Kim et al., 2009). No differences were observed between any of the cuprizone treatment groups and the non-treated group with regard to the number of NeuN positive cells per microscopic field (76.5±4.8, 69.75±5.8, 71±4.1, and 78.5±6.8 NeuN positive cells per microscopic field for untreated, 3 week treated, 5 week treated and 5+3 weeks treated respectively) (Figure4). Importantly, these findings strongly indicate that cuprizone treatment did not induce neuronal cell death in the cortical layer V consistent with the idea that the observed demyelination observed with the

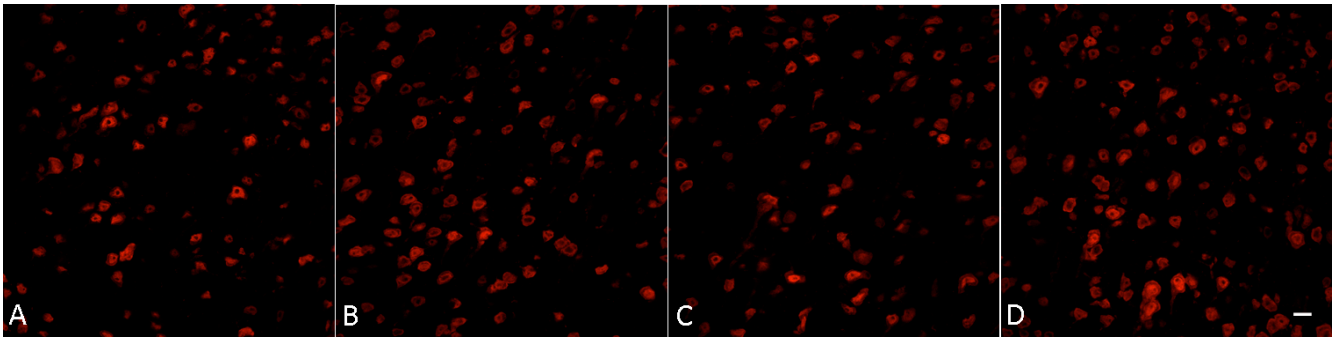

Figure 4. Cell death was not observed among treatments. NeuN, a neuronal cell marker, was used to quantify neuronal number in layer V of the cortex before (A, no cuprizone treatment), during (B, 3 week treated; C, 5 week treated) and after (D, 5 week treated, 3 weeks recovery. Scale bar: 15 μm

MBP labeling was not a consequence of neuronal death with subsequent axon degeneration.

The extent of axonal pathology did not differ among treatments

Our findings with NeuN strongly indicate that neuronal cell death was not prevalent in the cuprizone treated mice; however, more subtle neuronal pathologies could potentially be caused by the toxic effect of cuprizone, which might compromise AIS integrity independent of myelin loss. To further explore this possibility, we used immunolabeling to assess pathologies associated with the neuronal cytoskeleton and axonal transport. Previous studies have used the SMI-32 antibody, an antibody that recognizes non-phosphorylated neurofilaments, as an indicator of axonal cytoskeletal pathology (Trapp et al., 1998). In the mature axon, neurofilaments are extensively phosphorylated and the loss of this phosphorylation is indicative of compromised cytoskeletal integrity. As shown in Figure 5, minimal reactivity against SMI-32 was observed in all of the mice and no difference between the treated (Figure 5B-D) and untreated (Figure 5A) groups was observed. These findings demonstrate that the state of neurofilament phosphorylation was not altered with cuprizone exposure.

Although the findings from the SMI-32 labeling indicated that the cytoskeleton was not compromised, neuronal health was further assessed by labeling the cortical layer V with an antibody directed against amyloid precursor protein (APP). APP is a protein that is normally expressed by CNS neurons and is transported along the axon (Koo et al., 1990).

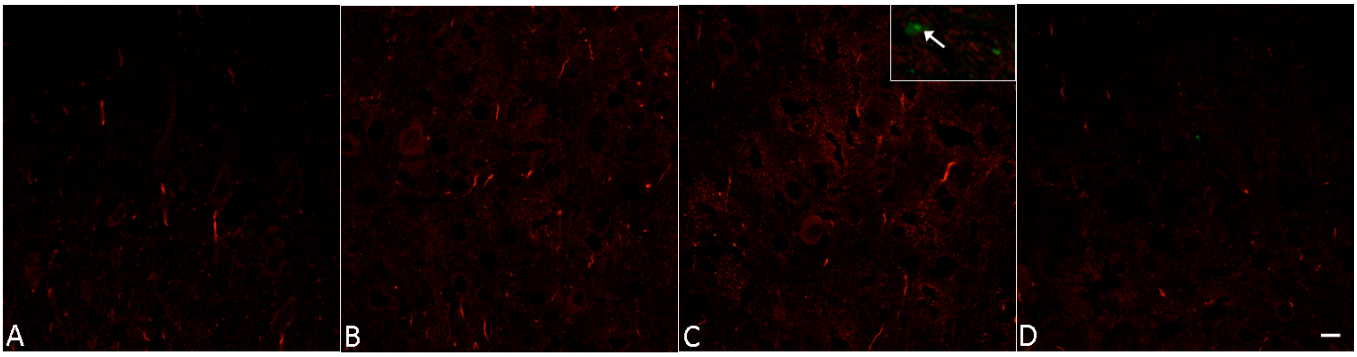

Figure 5. The extent of axonal pathology did not differ among treatments. Markers of axonal pathology, amyloid precursor protein (APP, green) and SMI 32 (anti-dephosphorylated neurofilaments, red), revealed no pathology in cortical layer V neurons among any of the treatment paradigms (A, no cuprizone treatment; B, 3 week treated; C, 5 week treated; D, 5 weeks treated, 3 weeks recovery). Consistent with previous studies axonal pathology as indicated by APP labeling was observed in the corpus callosum (inset). Scale bar: 10 μm

Therefore, the expression of APP is not pathological; however, accumulations of this protein within the axon are indicative of compromised axonal transport and subsequently, compromised axonal health. As shown in Figure 5, APP positive accumulations were not observed in the cortical layer V consistent with unimpaired axonal transport. Although APP accumulations were not observed in the cortical layer V, APP accumulations were observed in the corpus callosum of the mice treated with cuprizone for 5 weeks (Figure 5, inset). The presence of these accumulations in the corpus callosal axons in cuprizone treated mice is consistent with previous studies (Tsiperson et al., 2010; Skripuletz et al., 2013) further confirming the validity of our cuprizone treatment and that the lack of APP labeling in the cortex was not due to technical error. Importantly, a qualitative assessment of APP accumulations indicated that these pathologic markers were dramatically less prevalent in the corpus callosum of mice that were treated with cuprizone for 5 weeks followed by an additional 3 weeks of recovery. The reduction in the frequency of APP accumulations is consistent with axonal recovery subsequent to toxin withdrawal. Together, these findings suggest that neuronal toxic effects from cuprizone treatment were minimal.

Caspr clustering reveals nodes of Ranvier and distal end of AIS

To quantify the integrity of the AIS in mice following demyelination, cortical sections were immunolabeled with an antibody directed against AnkG, an AIS marker (Buffington and Rasband, 2011). Although the AnkG antibody provided robust labeling of the AIS, small structures not consistent with AIS in longitudinal orientation were also observed. In

coronal sections, the AIS of cortical layer V should be cut in longitudinal orientation; however, to determine whether these small, ankG-labeled structures were AIS cut in cross section, cortical sections were double labeled with antibodies directed against AnkG and caspr, a paranodal marker (Bhat et al., 2001)). Caspr was chosen since ankG also clusters in nodes of Ranvier (Buffington and Rasband, 2011). If the small, ankG labeled structures were nodes of Ranvier, then the caspr labeling would bracket the ankG labeling consistent with the paranode-node-paranode structure. As shown in Figure 6, qualitative analysis of the caspr/AnkG double-labeled sections confirmed the presence of nodal clusters as caspr labeling appeared as two adjacent accumulations separated by a small ankG labeled region, corresponding to the node of Ranvier (Figure 6A). Consistent with demyelination, both ankG nodal labeling and caspr paranodal labeling were reduced following 5 weeks of cuprizone treatment (Figure 6B).

AIS Analysis

As the above analysis revealed, the cuprizone model was successful in eliciting demyelination with minimal toxic effects on the axon. To analyze AIS integrity following demyelination, an antibody directed against ankG was used to identify the AIS of the cortical neurons of layer V. Using the image analysis software, Volocity™ (Perkin-Elmer, Waltham, MA), number, length and area of AIS were determined. These values were compared against their untreated groups as percentages of controls (untreated). All values are shown in Tables IV and VI. ImageJ was also used to quantify number and length of AIS as shown in Tables V and VII. The number of AIS in the medial region of the cortex,

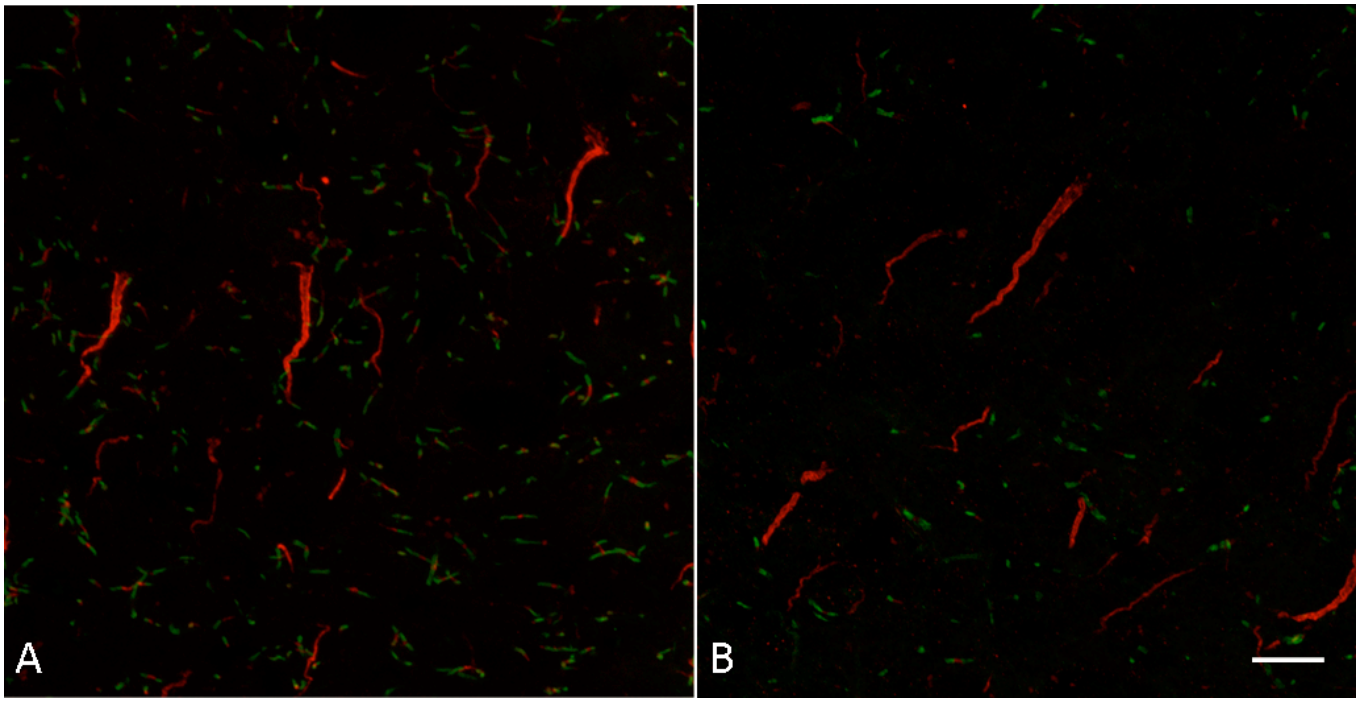

Figure 6. Nodes of Ranvier decrease following cuprizone treatment. Caspr (green), a known paranodal marker, was used to qualitatively assess the control levels of nodes, labeled with an antibody against the known AIS and node protein, ankyrinG (red; A, 5 week untreated) and the breakdown of nodes following cuprizone treatment (B, 5 week treated). Scale bar: 10 μm

as compared using Volocity™ , appeared to be consistently reduced; however, statistical analysis determined that these apparent reductions were no significantly different (p=0.44, 0.30 and 0.39 for 3, 5 an 5+3 weeks, respectively) (Tables IV and V). In support of this conclusion, ImageJ analysis of the number of AIS confirmed no difference between treated and untreated mice for any of the treatment groups. Similarly, the number of AIS, as analyzed by Volocity™, observed in the lateral region of cortical layer V showed no difference between treated and untreated groups(p= 0.78, 0.81 and 0.07 for 3, 5 an 5+3 weeks, respectively). Consistent with analysis of the medial cortex, the analysis of the lateral cortical region with ImageJ confirmed that neither the number nor the length of the AIS was significantly different between untreated and treated groups for the lateral regions of cortical layer V (Tables VI and VII). Previous work (Mason et al., 2001) has shown that axonal caliber changes with demyelination and remyelination; therefore, we measured the surface area of AIS as an indicator of axon caliber. Our data indicated no significant change in the average surface area of the AIS from either the medial or lateral regions of cortical layer V between mice maintained on normal and cuprizone containing chow.

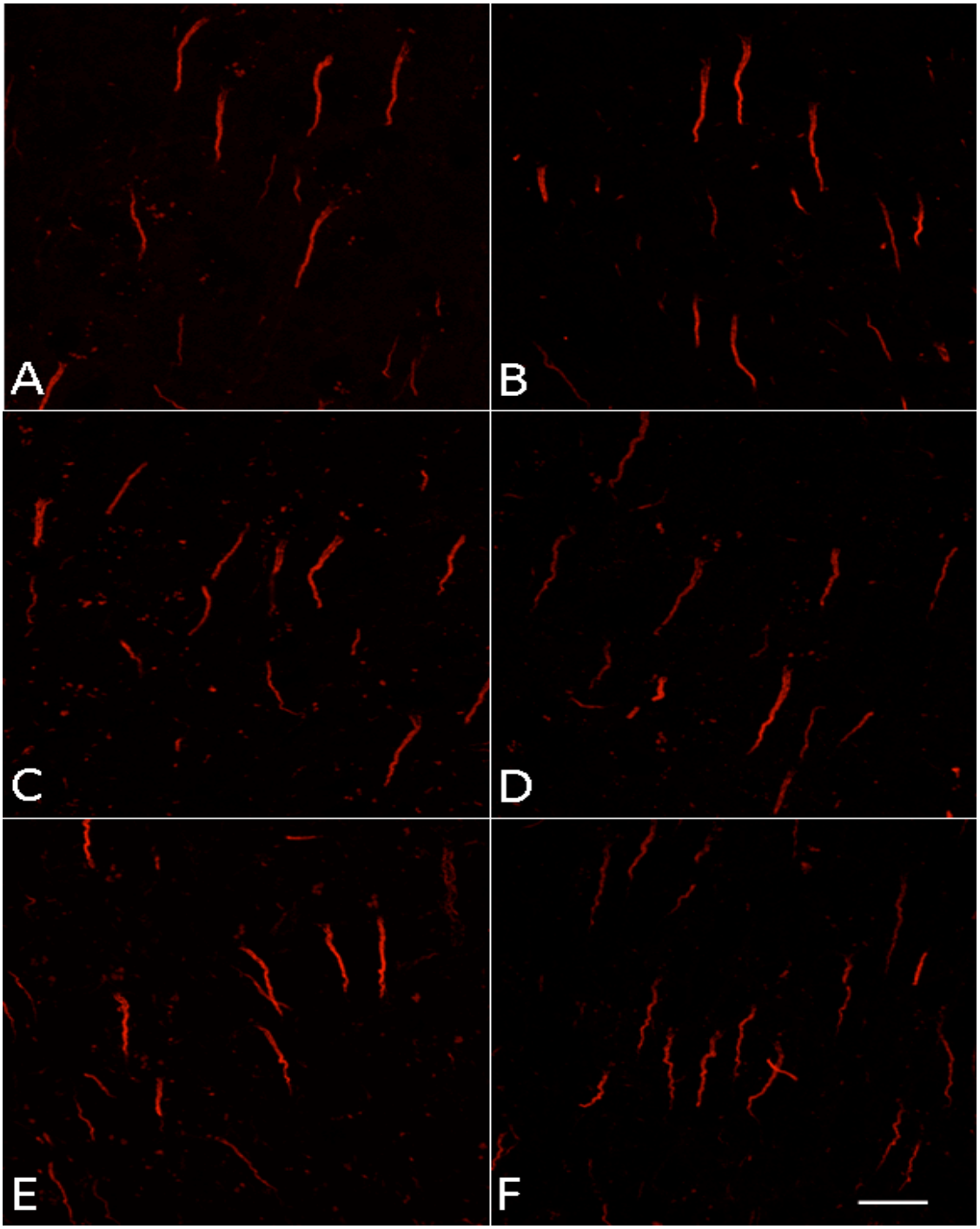

Figure 7. AnkG labeling of axon initial segments revealed no significant difference in number, length or surface area following demyelination in the medial region of cortex. Cortical sections immunolabeled with ankG revealed robust labeling of medial cortical layer V neurons in both cuprizone treated (B, 3 week; D, 5 week; F, 5 week, 3 weeks recovery) and untreated (A, 3 week; C, 5 week; E, 5 week) mice. Volocity™ and ImageJ analysis revealed no significant difference in number, length or surface area. Scale bar: 15 μm

Quantitative analysis of medial cortex using Volocity™

	3 week		5 week		5+3 week	
	No cup	Cup	No cup	Cup	No Cup	Cup
Number	100±19.3	77.5±23.8	100±35.7	50.5±40.6	100±22.9	66.7±40.3
Length (μm)	100±14.7	67.3±9.8	100±26.8	98.2±47.8	100±37.0	119.7±32.4
Surface Area (μm^2)	100±9.0	84.3±9.9	100±17.0	90.6±27.7	100±13.6	107.8±28.7

Table IV. Number, length (μm) and surface area (μm^2) of medially located AIS reported from Volocity™ calculated as percentages ± SEM

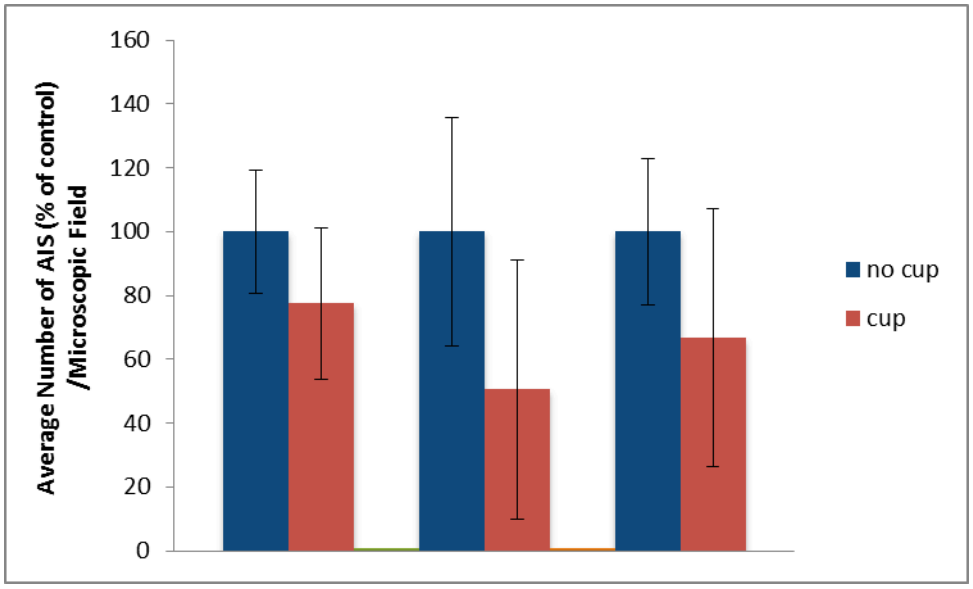

Figure 8. Number of axon initial segments was not significantly changed following demyelination in medial cortex. Although the average number of initial segments in layer V for all treatment groups appeared reduced as compared to mice maintained on normal chow, the differences were not significant. Data are presented as mean percent of control ± SEM.

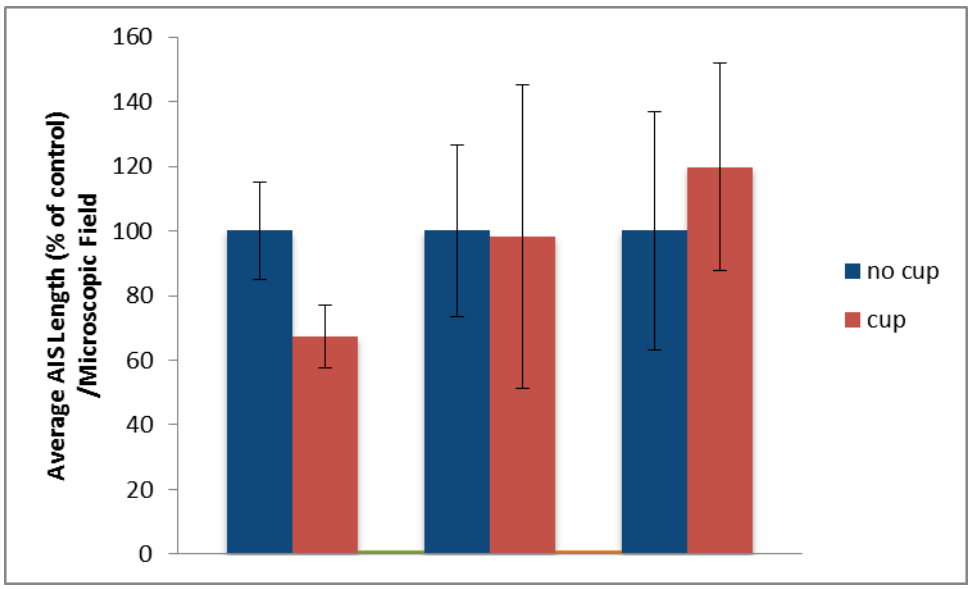

Figure 9. Length of axonal initial segments was not altered following demyelination in medial cortex. Data are presented as mean percent of control ± SEM.

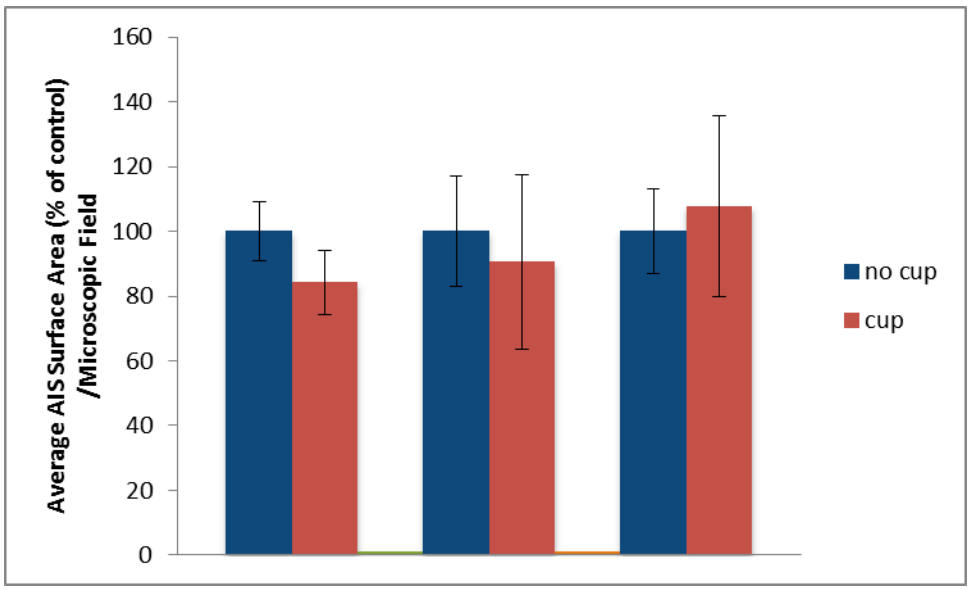

Figure 10. Surface area of axon initial segments was not changed following demyelination in medial cortex. Data are presented as mean percent of control ± SEM.

Quantitative analysis of medial cortex using ImageJ

	3 week		5 week		5+3 week	
	No cup	Cup	No cup	Cup	No Cup	Cup
AIS Number	220.7±35.0	193.0±34.6	195.3±37.0	191.7±22.1	216.3±32.7	188.0±27.3
AIS Length	17.6±1.0	17.1±1.5	15.4±0.7	15.9±0.6	14.1±0.8	14.5±0.1

Table V. Number and length of medially located AIS. Using Image J, neither the number nor the average length of cortical layer V AIS was significantly different between cuprizone treated and untreated mice. Data presented as mean ± SEM

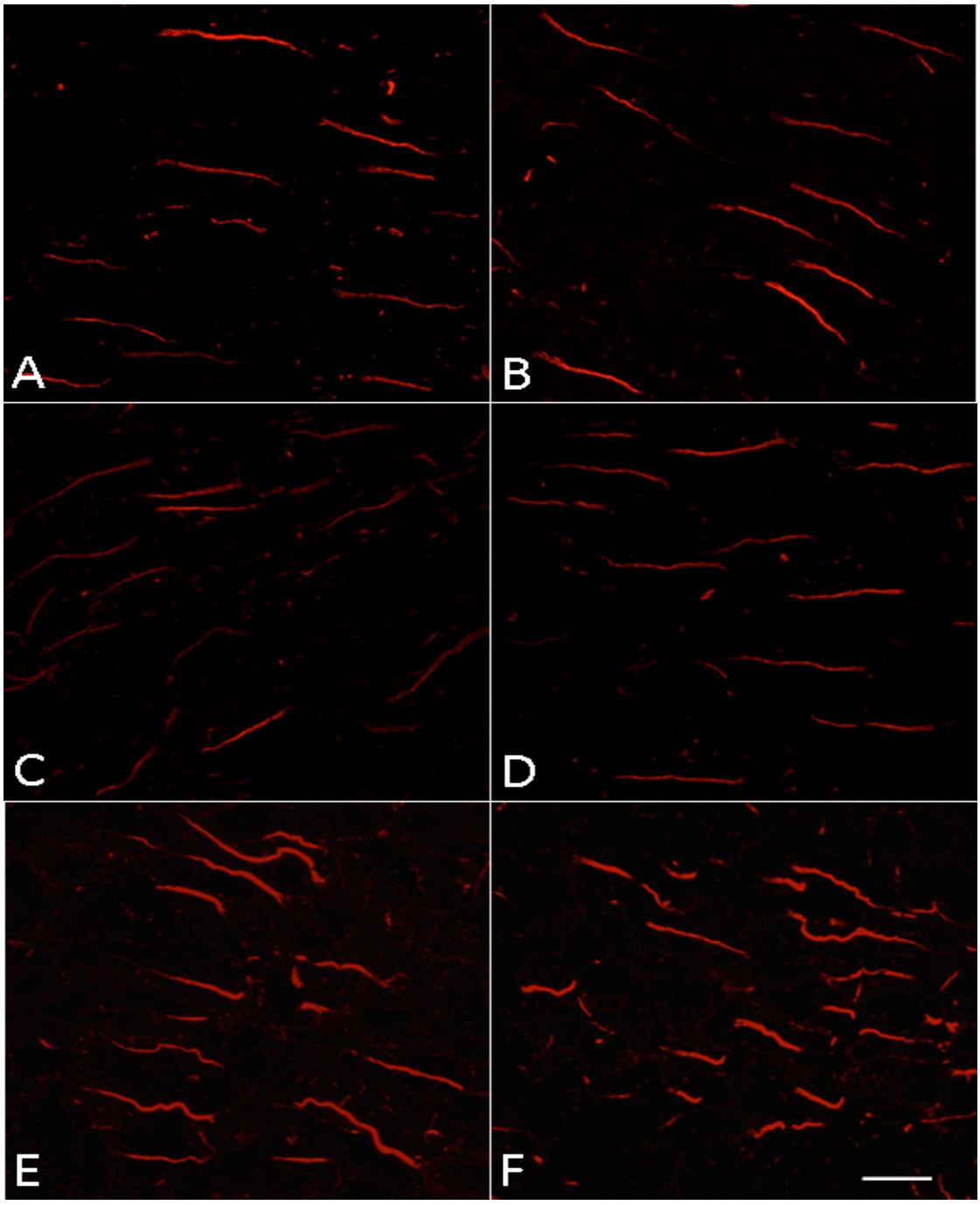

Figure 11. AnkG labeling of axon initial segments revealed no significant change in number, length or surface area following demyelination in lateral cortex. Cortical sections immunolabeled with ankG revealed robust labeling of lateral cortical layer V neurons in both cuprizone treated (B, 3 week; D, 5 week; F, 5 week, 3 weeks recovery) and untreated (A, 3 week; C, 5 week; E, 5 week) mice. Volocity™ and ImageJ analysis revealed no significant difference in number, length or surface area. Scale bar: 15 μm

Quantitative analysis of lateral cortex using Volocity™

	3 week		5 week		5+3 week	
	No cup	Cup	No cup	Cup	No Cup	Cup
Number	100±14.4	106.2±19.5	100±15.9	92.7±3.2	100±7.6	113.8±6.7
Length (μm)	100±28.5	91.2±23. 6	100±23.5	128.5±34.6	100±12.3	113.5±17.4
Surface Area (μm^2)	100±4.0	44.8±36.4	100±39.9	60.8±21.7	100±17.6	79.9±12.8

Table VI. Number, length (μm) and surface area (μm^2) of laterally located AIS reported from Volocity™ calculated as percentages of control ± SEM

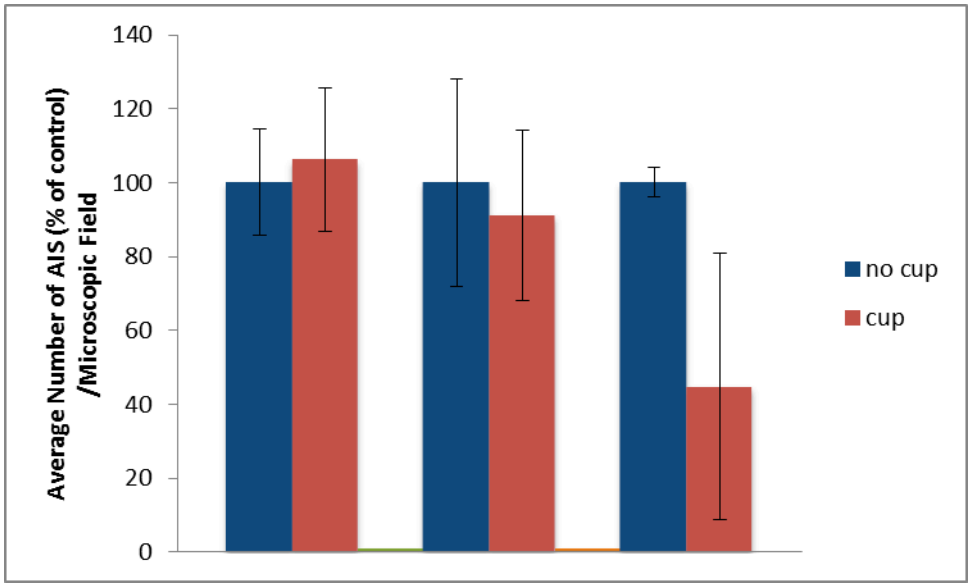

Figure 12. Number of axonal initial segments was not significantly changed following demyelination in lateral cortex. Data are presented as mean percent of control ± SEM.

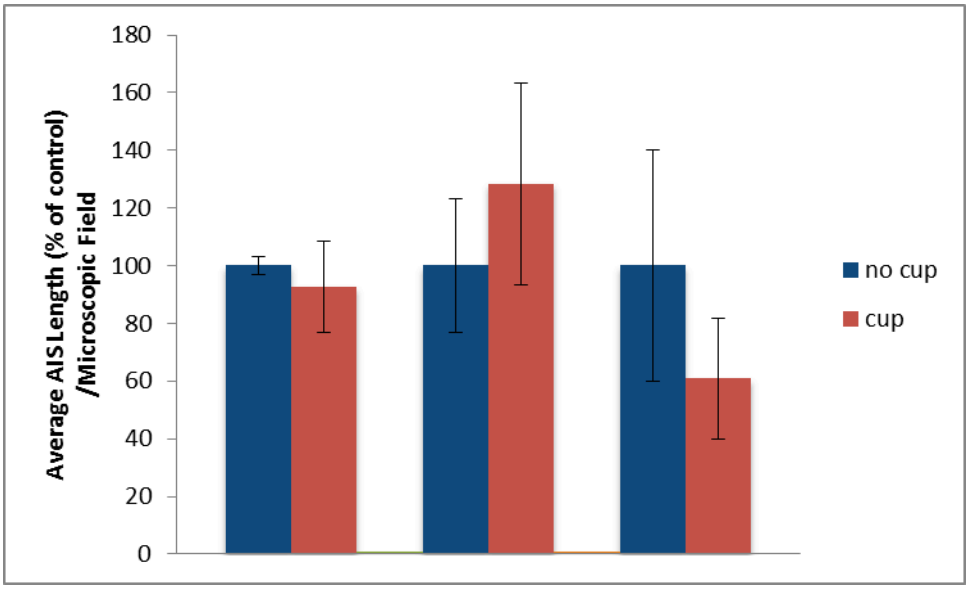

Figure 13. Length of axon initial segments was not changed following demyelination in lateral cortex. Data are presented as mean percent of control ± SEM.

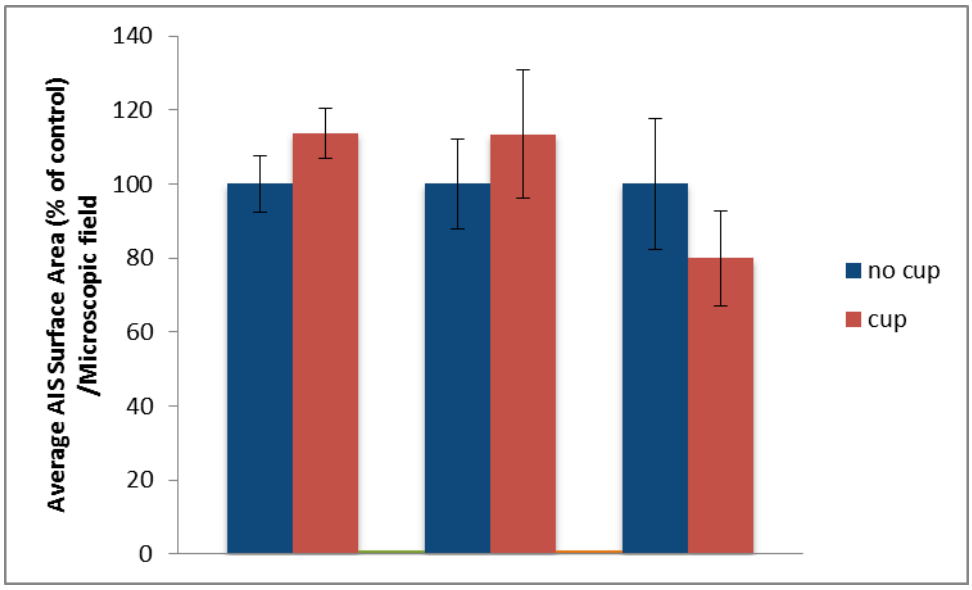

Figure 14. Surface area of axon initial segments was not changed following demyelination in lateral cortex. Data are presented as mean percent of control ± SEM.

Quantitative analysis of lateral cortex using ImageJ

	3 week		5 week		5+3 week	
	No cup	Cup	No cup	Cup	No Cup	Cup
AIS Number	248.0±42.4	216.3±31.4	199.0±38.1	233.3±12.5	206.7±4.1	185.3±33.6
AIS Length	18.9±1.1	19.2±0.1	19.0±0.2	19.1±1.2	17.2±0.6	18.0±0.7

Table VII. Counts and length of laterally located AIS ImageJ reported as mean ± SEM

Discussion

The goal of this study was to determine if maintenance of the myelin sheath is required for the preservation of AIS in CNS myelinated axons. While it is known that axon pathology is a major contributor to impaired motor, sensory and cognitive dysfunction associated with multiple sclerosis (Dutta and Trapp, 2011), the early events responsible for axonal pathology remain unclear. It is recognized that maintaining proper axonal function is intimately related to proper establishment and maintenance of axonal domains such as the node of Ranvier and the AIS (Bhat et al, 2001; Buttermore et al., 2013). Moreover, previous studies from our laboratory (Dupree et al., 1999; Dupree et al., 2004; Marcus et al., 2006; Pomicter et al., 2010) and others (Dugandžija-Novaković et al. 1995; Salzer et al., 1997; Rasband et al., 1998; Rasband et al., 1999; Tait et al., 2000; Bhat et al., 2001) have demonstrated that myelin contact is required for both the formation and maintenance of the node of Ranvier. However, formation of the AIS of myelinated axons does not require myelin axon contact (Zonta et al., 2011). Therefore, the node of Ranvier and the AIS, two axonal domains that cluster many of the same proteins (Buffington and Rasband, 2011), utilize different mechanisms for molecular formation. Presently, no study has

addressed whether myelin is required for maintaining the AIS. Here, we provide the first evidence that the myelin sheath is not essential for maintaining the integrity of the AIS.

To assess changes in AIS integrity, we analyzed AIS number, length and surface area of cortical neurons following demyelination. Previous studies have shown that the AIS is the site of action potential (AP) initiation (Stuart and Sakmann, 1994; Mainen et al., 1995). Therefore, any structural changes at the AIS would have an impact on the excitability of neurons and the circuits in which they function (Baalman et al., 2013). Key players in AIS function and AP initiation are the voltage gated sodium channels. In the AIS two forms predominate: the immature isoform known as $Na_v1.2$, which is clustered in the proximal end of the AIS and the mature isoform known as $Na_v1.6$, which is clustered in the distal end of the AIS (Buffington and Rasband, 2011). In addition to the sodium channels, other ion channels also participate in regulating AIS activity, although the precise interplay among these channels remains poorly understood (Popovic et al., 2011). However, it is recognized by most studies that physical properties of the AIS, including length and location (Colbert & Johnston, 1996; Khaliq & Raman, 2006; Palmer & Stuart, 2006; Kole et al. 2007; Shu et al. 2007), are critical to AIS function. Therefore, we elected to use a marker of the AIS that reveals the distribution of all classes of voltage gated sodium channels and to use this marker to quantify physical properties of the AIS.

In order to quantify the effects of myelin loss on AIS integrity, we utilized a well-established murine model of CNS demyelination/remyelination that induces minimal off

target toxic effects (Matsushima and Morell, 2001). Consistent with the requirements for this study, Skripuletz et al. (2008) reported that administration of 0.2% cuprizone initiated consistent cortical layer V demyelination while removal of cuprizone allowed for myelin replacement. Based on the Skripuletz et al. report (2008), C57/black6 mice were maintained on ground chow containing 0.2% cuprizone for 3 weeks, 5 weeks and 5 weeks followed by 3 weeks on non-cuprizone containing chow, which allowed for remyelination. Immunocytochemical labeling of an AIS cytoskeletal scaffolding protein, ankG (Buffington and Rasband, 2011), showed no significant difference in the number of AIS from either the medial or lateral regions of cortical layer V regardless of the treatment. Similarly, there was no difference in length or surface area of medially or laterally located initial segments among the treatments. We had proposed that the maintenance of the AIS of myelinated axons requires myelin-axon interactions and that re-establishment of these interactions would trigger the restoration of AIS integrity. However, our data suggest that maintenance of the AIS is not dependent on myelin contact. Importantly, these findings demonstrate that clusters of the same proteins along the same axon employs distinct mechanisms for maintaining the integrity of their specific domains.

Although neither the number nor structure of AIS was changed in the present study, other injury paradigms have resulted in significant changes in CNS AIS. Using a photothrombotic stroke model, Hinman et al. (2012) reported a significant shortening of AIS in the peri-infarct cortical regions. Moreover, the region of the AIS that exhibited the greatest structural change was the distal end, which has been proposed as the action

potential spike trigger zone (Popovic et al., 2011). Therefore, structural and molecular changes to this region may have profound effects on AIS and, ultimately, axonal function. Hinman et al. (2012) did not investigate potential mechanisms responsible for the AIS structural changes; however, they hypothesized that calpain mediated cleavage may be involved, which is consistent with a previous report by Schafer et al (2009).

In the earlier work of Schafer et al. (2009), the middle cerebral artery occlusion stroke model was employed. The ischemic injury resulted in rapid and complete disruption of AIS protein clustering including the loss of ion channels, ankG and βIV spectrin independent of neuronal cell death or axonal degeneration. Although AIS domains were severely altered, nodes of Ranvier remained intact. These authors proposed that elevated levels of intracellular calcium activated the calcium dependent cysteine proteinase calpain, which in turn cleaved ankG and βIV spectrin. Although these authors did not demonstrate an increase in intracellular calcium, calpain inhibition preserved AIS molecular organization.

Interestingly, in multiple sclerosis, Waxman and colleagues proposed that increased levels of calcium may result from reversing the Na^+/Ca^+ exchanger (Craner et al., 2004). In support of this proposal, these authors reported that along demyelinated axons in multiple sclerosis, $Na_v1.6$ and Na_v 1.2 channels are diffusely distributed. Moreover, they reported that these abnormally distributed $Na_v1.6$ channels produce a persistent Na^+ current that drives the Na^+/Ca^+ exchanger to import a damaging level of calcium inside the

demyelinated axons (Waxman, 2006). With this in mind, combined with the findings of Rasband and colleagues (Schafer et al., 2009), it is plausible to predict that demyelination, distal to the AIS, would result in altered Na ion channel function subsequently inducing an increase in axonal calcium levels and calpain mediated-cleavage of the axonal cytoskeleton and cytoskeletal scaffolding proteins. Based on the findings from the current study, this pathologic cascade is not initiated in the AIS merely by demyelination.

Although the administration of cuprizone recapitulates the demyelination aspect of MS, cuprizone does not mimic the T cell mediated inflammatory response of the disease (McMahon et al., 2001). Therefore, altered Na^+ channel distribution, which accompanies demyelination in MS as reported by Waxman et al. (2004), may require an additional pathologic event such as T cell mediated inflammation that is present in MS (Dittel, 2008) but absent in the cuprizone model (McMahon et al., 2001). Presently, this possibility is being tested in our lab and preliminary findings indicate altered AIS structure of the cortical layer V neurons in mice induced with EAE, a CNS inflammation model that is frequently used to study certain aspects of MS (Steinman and Zamvil, 2006).

In conclusion, although the node of Ranvier and AIS cluster the same proteins, we show that they have distinct mechanisms for maintenance. While myelin is necessary to establish and maintain the integrity of the node, the AIS is formed and maintained independent of myelin.

Literature Cited

Arroyo EJ, Scherer SS. 2000. On the molecular architecture of myelinated fibers. Histochem Cell Biol 113:1-18.

Baalman KJ, Cotton RJ, Rasband SN, Rasband MN. Blast Wave Exposure Impairs Memory and Decreases Axon Initial Segment Length. Journal of Neurotrauma epub ahead of print.

Bekku Y, Rauch U, Ninomiya Y, Oohashi T. 2009. Brevican distinctively assembles extracellular components at the large diameter nodes of Ranvier in the CNS. J Neurochem 108:1266-1276.

Bennett V, Baines AJ. 2001 Spectrin and ankyrin-based pathways: metazoan inventions for integrating cells into tissues. Physiol Rev 81:1353-1392.

Bennet V, Lambert S. 1999. Physiological roles of axonal ankyrins in survival of premyelinated axons and localization of voltage-gated sodium channels. J Neurocytol 28:303-318.

Berghs S, Aggujaro D, Dirkx R, Jr, Maksimova E, Stabach P, Hermel JM, Zhang JP, Philbrick W, Slepnev V, Ort T. 2000. BetaIV spectrin, a new spectrin localized at axon initial segments and nodes of Ranvier in the central and peripheral nervous system. Physiol Rev 81(2):871-927.

Bhat MA, Rios JC, Lu Y, Garcia-Fresco GP, Ching W, St. Martin M, Li J, Einheber S, Chesler M, Rosenbluth J, Salzer JL, Bellen HJ. 2001. Axon-glia interactions and the domain organization of myelinated axons requires neurexinIV/Caspr/Paranodin. Neuron 30:369-383.

Birgbauer E, Rao TS, Webb M. 2004. Lysolecithin induces demyelination in vitro in a cerebellar slice culture system. J Neurosci Res 78:157-66.

Bjartmar C, Yin X, Trapp BD. 1999. Axonal pathology in myelin disorders. J Neurocytol 28:383–395.

Blakemore W.1972. Observations on oligodendrocyte degeneration, the resolution of status spongiosus and remyelination in cuprizone intoxication in mice. J Neurocytol 1:413:426.

Blakemore W. 1973. Demyelination of the superior cerebellar peduncle in the mouse induced by cuprizone. J Neurol Sci 20:63-72.

Boiko T, Rasband MN, Levinson SR, Caldwell JH, Mandel G, Trimmer JS, Matthews G. 2001. Compact myelin dictates the differential targeting of two sodium channel isoforms in the same axon. Neuron 30:91–104.

Boiko T, Van Wart A, Caldwell JH, Levison SR, Trimmer JS, Matthews G. 2003. Functional specialization of the axon initial segment by isoform-specific sodium channel targeting. J Neurosci 27:2306–2313.

Boison D and Stoffel W. 1994. Disruption of the compacted myelin sheath of axons of the central nervous system in proteolipid protein-deficient mice. Proc Natl Acad Sci USA 91(24):11709-13.

Bo L, Vedeler CA, Nyland HI, Trapp BD, Mork SJ. 2003. Subpial demyelination in the cerebral cortex of multiple sclerosis patients. J Neuropathol Exp Neurol 9:323-331.

Brakebusch C, Seidenbecher CI, Asztely F, Rauch U, Matthies H, Meyer H, Krug M, Bockers TM, Zhou X, Kreutz MR, Montag D, Gundelfinger ED, Fässler R. 2002. Brevican-deficient mice display impaired hippocampal CA1 long-term potentiation but show no obvious deficits in learning and memory. Mol Cell Biol 22:7417–7427.

Buffington SA, Rasband MN. 2011. The axon initial segment in nervous system disease and injury. Euro J Neuro 34:1609-1619.

Buttermore ED, Piochon C, Wallace ML, Philpot BD, Hansel C, Bhat MA. 2012. Pinceau organization in the cerebellum requires distinct functions of Neurofascin in Purkinje and basket neurons during post-natal development. J Neurosci 32:4724-4742.

Buttermore ED, Thaxton CL, Bhat MA. 2013. Organization and Maintenance of Molecular Domains in Myelinated Axons. J Neurosci Res 91:603-622.

Caldwell JH, Schaller KL, Lasher RS, Peles E, Levinson SR. 2000. Sodium channel Nav1.6 is localized at nodes of ranvier, dendrites, and synapses. Proc Natl Acad Sci USA 97:5616-5620.

Cammer W, Zhang H. 1993. Atypical localization of the oligodendrocyte isoform (Pl) of glutathione-S-transferase in astrocytes during cuprizone intoxication. J Neurosci Res 36:183-190.

Colbert CM, Johnston D .1996. Axonal action-potential initiation and Na+ channel densities in the soma and axon initial segment of subicular pyramidal neurons. J Neurosci 16:6676–6686.

Coetzee T, Suzuki K, Nave KA, Popko B. 1999. Myelination in the absence of galactolipids and proteolipid proteins. Mol Cell Neurosci 14(1):41-51.

Craner MJ, Newcombe J, Black JA, Hartle C, Cuzner ML, Waxman SG. 2004. Molecular changes in neurons in multiple sclerosis: altered axonal expression of Nav1.2 and Nav1.6 sodium channels and Na+/Ca2+ exchanger. Proc Natl Acad Sci USA 101(21):8168-73.

Dal Canto MC, Lipton HL. 1980. Schwann cell remyelination and recurrent demyelination in the central nervous system of mice infected with attenuated Theiler's virus. Am J Pathol 98(1):101-22.

Dal Canto MC, Melvold RW, Kim BS, Miller SD. Two models of multiple sclerosis: experimental allergic encephalomyelitis (EAE) and Theiler's murine encephalomyelitis virus (TMEV) infection. A pathological and immunological comparison. Microsc Res Tech. 32(3):215-29.

Davis JQ, Lambert S, Bennett V. 1996. Molecular composition of the node of Ranvier: identification of anykrin-binding cell adhesion molecules neurofascin (mucin+/third FNIII domain-) and NrCAM at nodal axon segments. J Cell Biol 135:1355-1367.

Dittel BN. 2008. CD4 T cells: Balancing the coming and going of autoimmune-mediated inflammation in the CNS. Brain Behav Immun. 22(4):421-30.

Dugandzija-Novakovic S, Koszowski, AG, Levinson, SR, Shrager P. 1995. Clustering of Na channels and node of Ranvier formation in remyelinating axons. J Neurosci 15: 492–502.

Duncan ID, Hammang JP, Trapp BD. 1987. Abnormal compact myelin in the myelin-deficient rat: absence of proteolipid protein correlates with a defect in the intraperiod line. Proc Natl Acad Sci USA 84:6287–6291.

Dupree JL, Coetzee T, Blight A, Suzuki S, Popko B. 1998. Myelin galactolipids are essential for proper node of Ranvier formation in the CNS. J Neurosci 18:1642-1649.

Dupree JL, Girault JA, Popko B. 1999. Axo-glial interactions regulate the localization of axonal paranodal proteins. J Cell Biol 147(6):1145-1152.

Dupree JL, Mason JL, Marcus JR, Stull M, Levinson R, Matsushima GK, Popko B. 2004. Oligodendrocytes assist in the maintenance of sodium channel clusters independent of the myelin sheath. Neuron Glia Biol 1:179-192.

Dupree JL, Popko B. 1999. Genetic dissection of myelin galactolipid function. J Neurocytol 28:271-279.

Dutta R, McDonough J, Yin X, et al. 2006. Mitochondrial dysfunction as a cause of axonal degeneration in multiple sclerosis patients. Ann Neurol 59:478–489.

Dutta R, Trapp BD. 2010. Pathogenesis of axonal and neuronal damage in multiple sclerosis. Neurology 68:22-31.

Dutta R, Trapp BD. 2011. Mechanisms of Neuronal Dysfunction and Degeneration in multiple sclerosis. Prog Neurobiol 93(1):1-12.

Dzhashiashvili Y, Zhang Y, Galinska J, Lam I, Grumet M, Salzer JL. 2007. Nodes of Ranvier and axon initial segments are anykrin G-dependent domains that assemble by distinct mechanisms. J Cell Biol 177:857-870.

Eshed Y, Feinberg K, Poliak S, Sabanay H, Sarig-Nadir O, Spiegel I, Bermingham JR Jr, Peles E. 2005. Gliomedin mediates Schwann cell-axon interaction and the molecule assembly of the nodes of Ranvier. Neuron 47:215-229.

Feinberg K, Eshed-Eisenbach Y, Frechter S, Amor V, Salomon D, Sabanay H, Dupree JL, Grumet M, Brophy PJ, Shrager P, Peles E. 2010. A glial signal consisting of gliomedin and NrCAM clusters axonal Na+ channels during the formation of nodes of Ranvier. Neuron. 65(4):490-502.

Fujita N, Ishiguro H, Sato S, Kurihara T, Kuwano R, Sakimura K, Takahashi Y, Miyatake T. 1990. Induction of myelin-associated glycoprotein mRNA in experimental remyelination. Brain Res 513:152-155.

Gasser A, Ho TS, Chang KJ, Waxman SG, Rasband B, Peles E. 2002. Retention of cell adhesion complex at the paranodal junction requires the cytoplasmic region of Caspr. J Cell Biol 178:875-886.

Gollan L, Sabanay H, Poliak S, Berglund EO, Ranscht B, Peles E. 2002. Retention of a cell adhesion complex at the paranodal junction requires the cytoplasmic region of caspr. J Cell Biol 157(7):1247-56.

Gout O, Gansmuller A, Baumann N, Gumpel M. 1988. Remyelination by transplanted oligodendrocytes of a demyelinated lesion in the spinal cord of the adult shiverer mouse. Neurosci Lett 87(1-2):195-9.

Gumpel M, Baumann N, Raoul M, Jacque C. 1983. Survival and differentiation of oligodendrocytes from neural tissue transplanted into new-born mouse brain. Neurosci Lett 37(3):307-11.

Hall SM. 1972. The effects of injection of potassium cyanide into the sciatic nerve of the adult mouse: in vivo and electron microscopic studies. J Neurocytol. 1:233-54.

Hauser SL, Oksenberg JR. 2006. The Neurobiology of Multiple Sclerosis: Genes, Inflammation, and Neurodegeneration. Neuron 52: 61–76.

Hedstrom KL, Ogawa Y, Rasband MN. 2008. AnkyrinG is required for maintenance of the axon initial segment and neuronal polarity. *Jour Cell Biol* 183:635-640.

Hedstrom KL, Xu X, Ogawa Y, Frishknecht R, Seidencecher Cl, Shrager P, Rasband MN. 2007. Neurofascin assembles a specialized extracellular matrix at the axon initial segment. J Cell Biol 183:635-640.

Hickey WF, Hsu BL, Kimura H. 1991. T-lymphocyte entry into the central nervous system. J Neurosci Res 28:254–260.

Hinman JD, Rasband MN, Carmichael ST. 2012. Remodeling of the Axon Initial Segment After Focal Cortical and White Matter Stroke. Stroke 44:182-189.

Hiremath MM, Saito Y, Knapp GW, Ting JP, Suzuki K, Matsushima GK. 1998. Microglial/macrophage accumulation during cuprizone-induced demyelination in C57BL/6 mice. J Neuroimmunol 92:38-49.

Hohlfeld R. 1997. Biotechnological agents for the immunotherapy of multiple sclerosis. Principles, problems and perspectives. Brain 120:865–916

Hudson LD. 2004. Proteolipid protein gene. In RA Lazzarini (Ed.) Myelin biology and disorders. pp. 401-420.

Hu W, Tian C, Li T, Yang M, Hou H, Shu Y. 2009. Distinct contributions of Na(v)1.6 and Na(v)1.2 in action potential initiation and backpropagation. Nat Neurosci 12:996-1002.

Jung T, Höhn A, Grune T. 2010. Lipofuscin: Detection and Quantification by Microscopic Techniques. Advanced Protocols in Oxidative Stress II, Methods in Molecular Biology pp. 173-176.

Kaplan MR, Cho MH, Ullian EM, Ison LL, Levinson SR, Barres BA. 2001. Differential control of clustering of sodium channels Na_v 1.2 and Na_v 1.6 at developing CNS nodes of Ranvier. Neuron 30:105-119.

Kaplan MR, Meyer-Franke A, Lambert S, Bennett V, Duncan ID, Levinson SR, Barres BA. 1997. Induction of sodium channel clustering by oligodendrocytes. Nature. 386:724-728.

Kesterson JW, Carlton WW. 1971. Histopathologic and enzyme histochemical observations of the cuprizone-induced brain edema. Exper Mol Pathol 15:82-96.

Khaliq ZM, Raman IM .2006. Relative contributions of axonal and somatic Na+ channels to action potential initiation in cerebellar Purkinje neurons. J Neurosci 26:1935–1944.

Kim KK, Adelstein RS, Kawamoto S. 2009. Identification of Neuronal Nuclei (NeuN) as Fox-3, a New Member of the Fox-1 Gene Family of Splicing Factors. J Biol Chem 284:31052-31061.

Kole MHP, Letzkus JJ, Stuart GJ. 2007. Axon initial segment Kv1 channels control axonal action potential waveform and synaptic efficacy. Neuron 55:633–647.

Komoda M, Soriano P. 2002. βIV-spectrin regulates sodium channel clustering through ankyrin-G at axon initial segments and nodes of Ranvier. J Cell Biol 156:337-348.

Komoly S, Jeyasingham MD, Pratt OE, Lantos PL. 1987. Decrease in oligodendrocyte carbonic anhydrase activity preceding myelin degeneration in cuprizone induced demyelination. J Neurol Sci 84:223-237.

Koo EH, Sisodia SS, Archer DR, Martin LJ, Weidemann A, Beyreuther K, Fischer P, Masters CL, Price DL. 1990. Precursor of amyloid protein in Alzheimer disease undergoes fast anterograde axonal transport. Proc Natl Acad Sci USA 87:1561-1565.

Kordeli E, Davis J, Trapp B, Bennett V. 1990. An isoform of ankyrin is localized at nodes in myelinated axons central and peripheral nerves. J Cell Biol 110(4):1341-52.

Kuba H, Oichi Y, Ohmori, H. 2010. Presynaptic activity regulates Na+ channel distribution at the axon initial segment. Nature 465:1075-1078.

Kursula P. 2008. Structural properties of proteins specific to the myelin sheath. Amino Acids. 34(2):175-85.

Labasque M, Devaux JJ, Lévêque C, Faivre-Sarrailh C. 2011. Fibronectin type III-like domains of neurofascin-186 protein mediate gliomedin binding and its clustering at the developing nodes of Ranvier. J Biol Chem 286:42426-34.

Lacas-Gervais S, Guo J, Strenzke N, Scarfone E, Kolpe M, Jahkel M, De Camilli P, Moser T, Rasband MN, Solimena M. 2004. BetaIVsigma1 spectrin stabilizes the nodes of Ranvier and axon initial segments. J Cell Biol 166:983-990.

Lambert S, Davis JQ, Bennett V. 1997. Morphogenesis of the node of Ranvier: co-clusters of anykrin and anykrin-binding intergral proteins define early developmental intermediates. J Neurosci 17:7025-7036.

Liu MC, Akle V, Zheng W, Kitlen J, O'Steen B, Larner SF, Dave JR, Tortella FC, Hayes RL, Wang KK. 2006. Extensive degradation of myelin basic protein isoforms by calpain following traumatic brain injury. J Neurochem 98(3):700-12.

Lu F, Selak M, O'Connor J, et al. 2000. Oxidative damage to mitochondrial DNA and activity of mitochondrial enzymes in chronic active lesions of multiple sclerosis. J Neurol Sci 177:95–103

Ludwin SK. 1978. Central nervous system demyelination and remyelination in the mouse. An ultrastructural study of cuprizone toxicity. Lab Invest 39:597-612.

Mainen ZF, Joerges J, Huguenard JR, Sejnowski TJ. 1995. A model of spike initiation in neocortical pyramidal neurons. Neuron 15:1427-39.

Marcus J, Honigbaum S, Shroff S, Honke K, Rosenbluth J, Dupree JL. 2006. Sulfatide is essential for the maintenance of CNS myelin and axon structure. Glia 53(4):372-81.

Marcus J, Popko B. 2002. Galactolipids are molecular determinants of myelin development and axo-glial organization. Biochim Biophys Acta 1573(3):406-13.

Martini R, Schachner M. 1986. Immunoelectron microscopic localization of neural cell adhesion molecules (L1, N-CAM, and MAG) and their shared carbohydrate epitope and myelin basic protein in developing sciatic nerve. J. Cell Biol. 103*:* 2439–2448.

Mason JL, Langaman C, Morell P, Suzuki K, Matsushima GK. 2001. Episodic demyelination and subsequent remyelination within the murine central nervous system; changes in axonal caliber. Neuropathology and Applied Neurobiology 27:50-58.

Matsushima GK and Morell P. 2001. The neurotoxicant, cuprizone as a model to study demyelination and remyelination in the central nervous system. Brain Pathol 11(1):107-16.

McMahon EJ, Cook DN, Suzuki K, Matsushima GK. 2001. Absence of macrophage-inflammatory protein-1alpha delays central nervous system demyelination in the presence of an intact blood-brain barrier. J Immunol 167(5):2964-71.

Morell P, Barrett CV, Mason JL, Toews AD, Hostettler JD, Knapp GW, Matsushima GK. 1998. Gene expression in the brain during cuprizone-induced demyelination and remyelination. Mol Cell Nuerosci 12:220-227.

Morell P, Radin NS. 1969. Synthesis of cerebroside by brain from uridine diphosphate galactose and ceramide containing hydroxyl fatty acid. Biochemistry 8:506-512.

Norton WT, Cammer, W. 1984. Isolation and characterization of myelin. In: MorellP, editor. Myelin, 2nd ed, New York: Plenum Press. pp 147–180.

Novakovic SD, Levinson SR, Schachner M, Shrager P. 1998. Disruption and reorganization of sodium channels in experimental allergic neuritis. Muscle Nerve 21:1019-32.

Quarles RH, Morell P, McFarland H. 2006. Myelin formation, structure and biochemistry. In: Basic neurochemistry: Molecular, cellular, and medical aspects. Siegel GJ, Albers RW, Brady ST and others, editors. 7th ed. New York, Elsevier Academic Press. 51 p.

Palmer LM & Stuart GJ. 2006. Site of action potential initiation in layer V pyramidal neurons. J Neurosci 26:1854–1863.

Pattison IH, Jebbett JN. 1972. Clinical and histological observations on cuprizone toxicity and scrapie in mice. Res Vet Sci 12:378-380.

Peles E, Nativ M, Lustig M, Grumet M, Schilling J, Martinex R, Plowman GD, Schlessinger J. 1997. Identification of a novel contactin associated transmembrane receptor with multiple domains implicated in protein-protein interactions. EMBO 16:978-988.

Peles E, Salzar J. 2000. Molecular domains of myelinated axons. Curr Opin Neurob 10:558-565.

Peterson LK, Fujinami RS. 2007. Inflammation, Demyelination, Neurodegeneration and Neuroprotection in the Pathogenesis of Multiple Sclerosis. J Neuroimmunol. 184:37-44.

Pevear DC, Calenoff M, Rozhon E, Lipton HL. 1987. Analysis of the complete nucleotide sequence of the picornavirus Theiler's murine encephalomyelitis virus indicates that it is closely related to cardioviruses. J Virol 61(5):1507-16.

Pillai AM, Thaxton C, Pribisko AL, Cheng JG, Dupree JL, Bhat MA. 2009. Spatio-temporal ablation of myelinating glia-specific neurofascin (nfascnf155) in mice reveals gradual loss of paranodal axo-glial junctions and concomitant disorganization of axonal domains. J Neurosci Res 87(8): 1773–1793.

Poliak S, Gollan L, Martinez R, Custer A, Einheber S, Salzar JL, Trimmer JS, Shrager P, Peles E. 1999. Caspr2, a new member of the neurexin superfamily, is localized at the juxtaparanodes of myelinated axons and associates with K^+ channels. Neuron 24:1037-1047.

Pomicter AD, Shroff SM, Fuss B, Sato-Bigbee C, Brophy PJ, Rasband MN, Bhat MA, Dupree JL. 2010. Novel forms of neurofascin 155 in the central nervous system: alterations in paranodal disruption models and multiple sclerosis. Brain. 133:389-405.

Popovic MA, Foust AJ, McCormick DA, Zecevic D. 2011. The spatio-temporal characteristics of action potential initiation in layer 5 pyramidal neurons: a voltage imaging study. J Physiol (Lond) 589:4167-4187.

Popko B. 2000. Myelin galactolipids: mediators of axo-glial interactions? Glia 29:149-153.

Raine CS. 1984. Morphology of myelin and myelination. In: Myelin. Morell P, editor. 2nd ed. New York: Plenum Press. 1 p.

Rasband MN. 2008. Na^+ channels get anchored…with a little help. J Cell Bio 183:975-977.

Rasband MN, Peles E, Trimmer JS, Levinson SR, Lux SE, Shrager P. 1999. Dependence of nodal sodium channel clustering on paranodal axoglial contact in the developing CNS. J Neurosci 19:7516-7528.

Rasband MN, Trimmer JS, Schwarz TL, Levinson SW, Ellisman MH, Schachnew M, Shrager P. 1998. Potassium channel distribution, clustering, and function in remyelinating axons. J Neurosci 18:36-47.

Roos RP, Casteel N. 1992. Determinants of neurological disease induced by Theiler's murine encephalomyelitis virus. In Roos, R.P. (Ed.), Molecular Neurovirology, Humana Press, Totowa, NJ, pp. 283–318.

Rosenbluth J. 1995. Glial membrane and axonal junctions. Neuroglia. New York: Oxford University Press; 613-633.

Salzar JL. 1997. Clustering sodium channels at the node of Ranvier: close encounters of the axon-glia kind. Neuron 18:843-846.

Salzer JL. 2003. Polarized domains of myelinated axons. Neuron 40:297-318.

Schafer DS, Jha S, Liu F, Akella T, McCullough LD, Rasband MN. 2009. Disruption of the axon initial segment cytoskeleton is a new mechanism for neuronal injury. J Neurosci 29: 13242–13254.

Schafer DS, Rasband MN. 2006. Glial regulation of the axonal membrane at nodes of Ranvier. Curr Opin Neurobiol 16:508-514.

Schnaar RL. 2010. Brain gangliosides in axon-myelin stability and axon regeneration. FEBS Letter 584:1741–1747.

Skripuletz T, Hackstette D, Bauer K, Gudi V, Rul R, Voss E, Berger K, Kipp M, Baumgartner W, Stangel M. 2013. Astrocytes regulate myelin clearance through recruitment of microglia during cuprizone induced demyelination. Brain 136:147-167.

Skripuletz T, Lindner M, Kotsiari A, Garde N, Fokuhl J, Linsmeier F, Trebst C, Stangel M. 2008. Cortical demyelination is prominent in the murine cuprizone model and is strain-dependent. Am J Path 172(4):1053-1061.

Sherman DL, Tait S, Melrose S, Johnson R, Zonta B, Court FA, Macklin WB, Meek S, Smith AJ, Cottrell DF, Brophy PJ. 2005. Neurofascins are required to establish axonal domains for saltatory conduction. Neuron 48:737–42.

Shu Y, Duque A, Yu Y, Haider B, McCormick DA. 2007. Properties of action potential initiation in neocortical pyramidal cells: evidence from whole cell axon recordings. J Neurophysiol 97:746–760.

Stadelmann C, Albert M, Wegner C, Bruck W. Cortical pathology in multiple sclerosis. 2008. Curr Opin Neurol 21(3):75-85.

Stecca B, Southwood CM, Gragerov A, Kelley KA, Friedrich VL Jr, Gow A. 2000. The evolution of lipophilin genes from invertebrates to tetrapods: DM-20 cannot replace proteolipid protein in CNS myelin. J Neurosci 20(11):4002-10.

Steinman L, Zamvil SS. 2006. How to successfully apply animal studies in experimental allergic encephalomyelitis to research on multiple sclerosis. Ann Neurol 60:12-21.

Sternberger NH, Quarles RH, Itoyama Y, Webster HD (1979) Myelin-associated glycoprotein demonstrated immunocytochemically in myelin and myelin-forming cells of developing rat. Proc Natl Acad Sci USA 76: 1510–1514.

Stidworthy MF, Genoud S, Suter U, Mantei N, Franklin RJ. 2003. Quantifying the early stages of remyelination following cuprizone-induced demyelination. Brain Pathol 13:329-39.

Stuart GJ, Sakmann B. Active propagation of somatic action potentials into neocortical pyramidal cell dendrites. Nature 367:69-72.

Suzuki K, Kikkawa T. 1969. Status spongiosus of CNS and hepatic changes induced by cuprizone (biscyclohexanone oxalyldihydrazone). Am J Pathol 54:307-325.

Tait S, Gunn-Moore F, Collinson JM, Huang J, Lubetzki C, Pedraza L, Sherman DL, Colman DR, Brophy PJ. 2000. An oligodendrocyte cell adhesion molecule at the site of assembly of the paranodal axo-glial junction. J Cell Biol 150(3):657-66.

Thaxton C, Bhat MA. 2009. Myelination and Regional Domain Differentiation of the Axon. Results Probl Cell Differ 48:1-28.

Thaxton C, Pillai AM, Pribisko AL, Dupree JL, Bhat MA. 2011. Nodes of Ranvier act as barriers to restrict invasion of flanking paranodal domains in myelinated axons. Neuron 69(2):244-57.

Traka M, Goutebroze L, Denisenko N, Bessa M, Nifli A, Havaki S, Iwakura Y, Fukamauchi F, Watanabe K, Soliven B, et al., 2003. Association of TAG-1 with Caspr2 is essential for the molecular organization of juxtaparanodal regions of myelinated fibers. J Cell Biol 162(6):1161-72.

Trapp BD, Nave KA. 2008. Multiple sclerosis: an immune or neurodegenerative disorder? Annu Rev Neurosci 31:247-269.

Trapp BD, Peterson J, Ransohoff RM, Rudick R, Mörk S, Bö L. 1998. Axonal transection in the lesions of multiple sclerosis. N Engl J Med 338:278-285.

Tsiperson V, Li X, Schwartz GJ, Raine CS, Shafit-Zagardo B. 2010. GAS6 Enhances Repair Following Cuprizone-Induced Demyelination. PLoS ONE 5(12):e15748.

Vabnick I, Shrager P. 1998. Ion Channel Redistribution and Function during Development of the Myelinated Axon. J Neurobiol 37:80-96.

Vabnick I, Trimmer JS, Scwarz TL, Levinson SR, Risai D, Shrager P. 1999. Dynamic potassium channel distributions during axonal development prevent aberrant axonal firing patterns. J Neurosci 19:747-758.

Vanderlugt CL, Miller SD. 2002. Epitope spreading in immune-mediated diseases: Implications for immunotherapy. Nat Rev Immunol 2:85–95.

Van Wart A, Matthews G. 2006. Impaired firing and cell-specific compensation in neurons lacking Nav1.6 sodium channels. J Neurosci 26:7172-7180.

Venturini G. 1973. Enzymatic activities and sodium, potassium and copper concentrations in mouse brain and liver after cuprizone treatment in vivo. J Neurochem 21:1147-1151.

von Herrath MG, Fujinami RS, Whitton JL. 2003. Microorganisms and autoimmunity: making the barren field fertile. Nat Rev Microbiol 1:151–157.

Wang H, Kunkel DD, Martin TM, Schwartzkroin PA, Tempel BL. 1993. Heteromultimeric K+ channels in terminal and juxtaparanodal regions of neurons. Nature 365(6441):75-79.

Waxman SG. 2006. Axonal conduction and injury in multiple sclerosis: the role of sodium channels. Nat Rev Neurosci. 7(12):932-41.

Waxman SG, Craner MJ, Black JA. 2004. Na+ channel expression along axons in multiple sclerosis and its models. Trends Pharmacol Sci 25(11):584-91.

Wekerle H, Sun D, Oropeza-Wekerle RL, Meyermann R. 1987. Immune reactivity in the nervous system: modulation of T-lymphocyte activation by glial cells. J Exp Biol 132:43–57.

Woodruff RH, Franklin RJ. 1999. Demyelination and remyelination of the caudal cerebellar peduncle of adult rats following stereotaxic injections of lysolecithin, ethidium bromide, and complement/anti-galactocerebroside: a comparative study. Glia 25(3):216-28.

Yang Y, Lacas-Gervais S, Moreset DK, Solimena M, Rasband MN. 2004. BetaIV spectrins are essential for membrane stability and the molecular organization of nodes of Ranvier. J Neurosci 24:7230-7240.

Yang Y, Ogawa Y, Hedstrom KL, Rasband MN. 2007. β-IV spectrin is recruited to axon initial segments and nodes of Ranvier by ankyrinG. J Cell Biol 176:509-519.

Zamvil SS, Steinman L. 2003. Diverse targets for intervention during inflammatory and neurodegenerative phases of multiple sclerosis. Neuron 38:685–688.

Zhou D, Lambert S, Malen PL, Carpenter S, Boland LM, Vann Bennett. 1998. AnkyrinG Is Required for Clustering of Voltage-gated Na Channels at Axon Initial Segments and for Normal Action Potential Firing. J Cell Biol 143(5): 1295–1304.

Zonta B, Desmazieres A, Rinaldi A, Tait S, Sherman DL, Nolan MF, Brophy PJ. 2011. A critical role for Neurofascin in regulating action potential initiation through maintenance of the axon initial segment. Neuron 69(5):945-56.

VITA

Anne Marie Josephson was born in Fairfax, Virginia, on July 19, 1989. She graduated from Bishop O'Connell High School, Arlington, Virginia in 2007. She received her Bachelor of Science degree in Biology from James Madison University, Harrisonburg, Virginia in 2011. She also received her Pre-Medical Graduate Health Sciences Certificate from Virginia Commonwealth University, Richmond, Virginia in 2012.